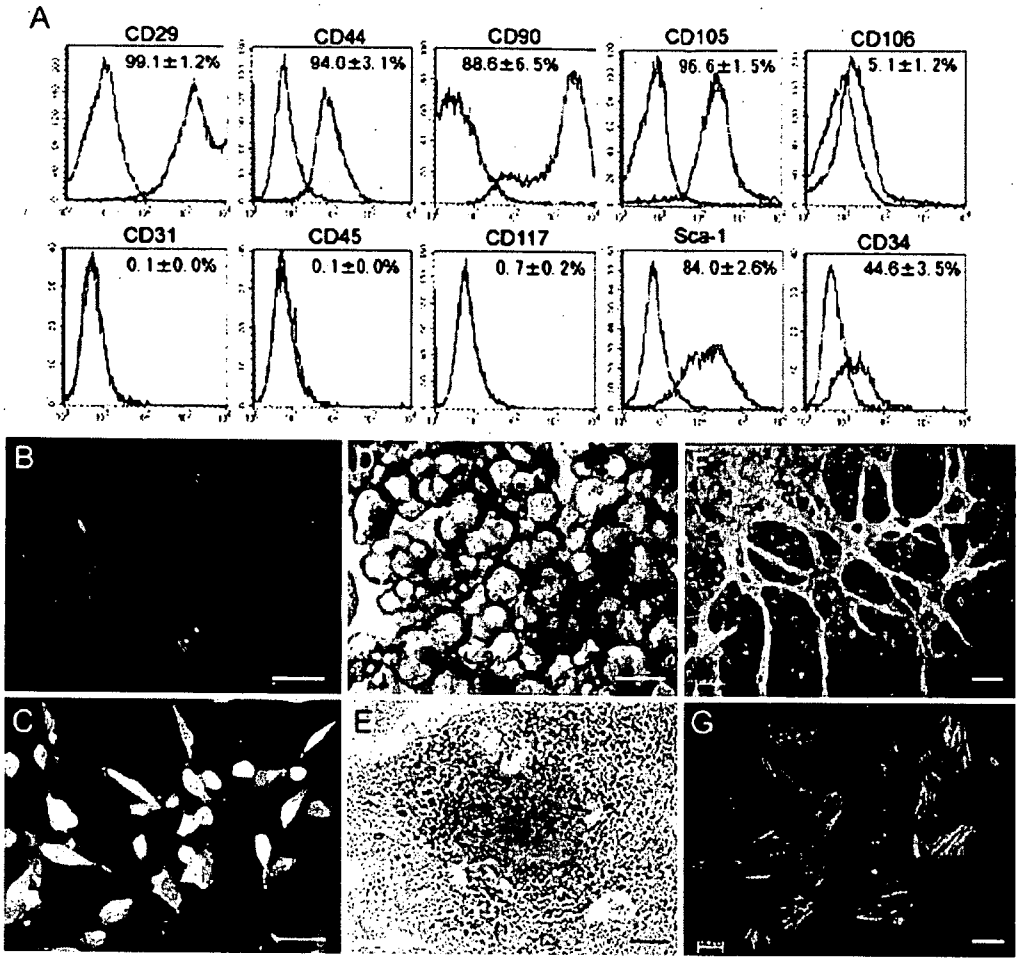

Fig. 2. MDPCs have mesenchymal cell-like phenotype and differentiate into endothelial and smooth muscle cells. (A) FACS analysis of MDPCs. Isotype controls were overlaid (blue lines) on each antigen tested (red lines). Immunostaining of mesenchymal markers on undifferentiated MDPCs. Vimentin (B, red) and type I collagen (C, green) are shown. DAPI (blue). Adipogenic- and osteogenic-inductions were verified by Oil red O (D, red) and Alizarin red (E, red), respectively. MDPCs were also induced into $CD31^+$ endothelial (F, green) and Sm-MHC^+ smooth muscle cells (G, red) by specific medium. DAPI (blue) Scale bars represent 50 μm in (E) and 20 μm in (B–D, F, and G).

MDPCs regenerate vascular smooth muscle cells with the restoration of δ-SG expression in vivo

We next generated δ-SG KD mice as a cardiomyopathy model by targeting δ-SG transcripts with an efficient KD vector, pDECAP-δ-SG [14]. Compared with non-transgenic littermates (NTG), the δ-SG expression on the membrane of cardiac muscle was disrupted in 28-week-old δ-SG KD mice (Fig. 3A left panels). The δ-SG expression along the vessels was also decreased, resulting in narrow vascular lumens with constrictive morphology (Fig. 3A middle panels). Masson's trichrome staining demonstrated extensive fibrosis surrounding the vessels (Fig. 3A right panels).

To determine whether MDPC transplantation can restore the δ-SG expression as well as regenerate the degenerated vessels in δ-SG KD hearts, a half million MDPCs transduced with a LacZ reporter gene were directly injected into three individual sites of myocardium. All transplanted hearts showed substantial $LacZ^+$ cell engraftment 4 weeks after implantation. $LacZ^+$ vascular smooth muscle cells could be readily detectable (Fig. 3B), and those were co-localized with δ-SG expression to regenerate new vessels (Fig. 3C arrows).

Transplantation of MDPCs improves cardiac function partially through the paracrine effectors production

We next asked whether MDPCs might restore δ-SG expression during differentiation process and found that MDPCs expressed δ-SG transcripts through smooth muscle cell lineage induction in vitro (Fig. 4A). A significant neoangiogenesis in the MDPC-injected area was observed in the MDPC-transplanted group compared with that in PBS-treated hearts (Fig. 4B). Cardiac function at baseline of δ-SG KD and NTG littermates was analyzed by echocardiography and showed a significant increase in LVDd and impaired systolic and diastolic functions in δ-SG KD

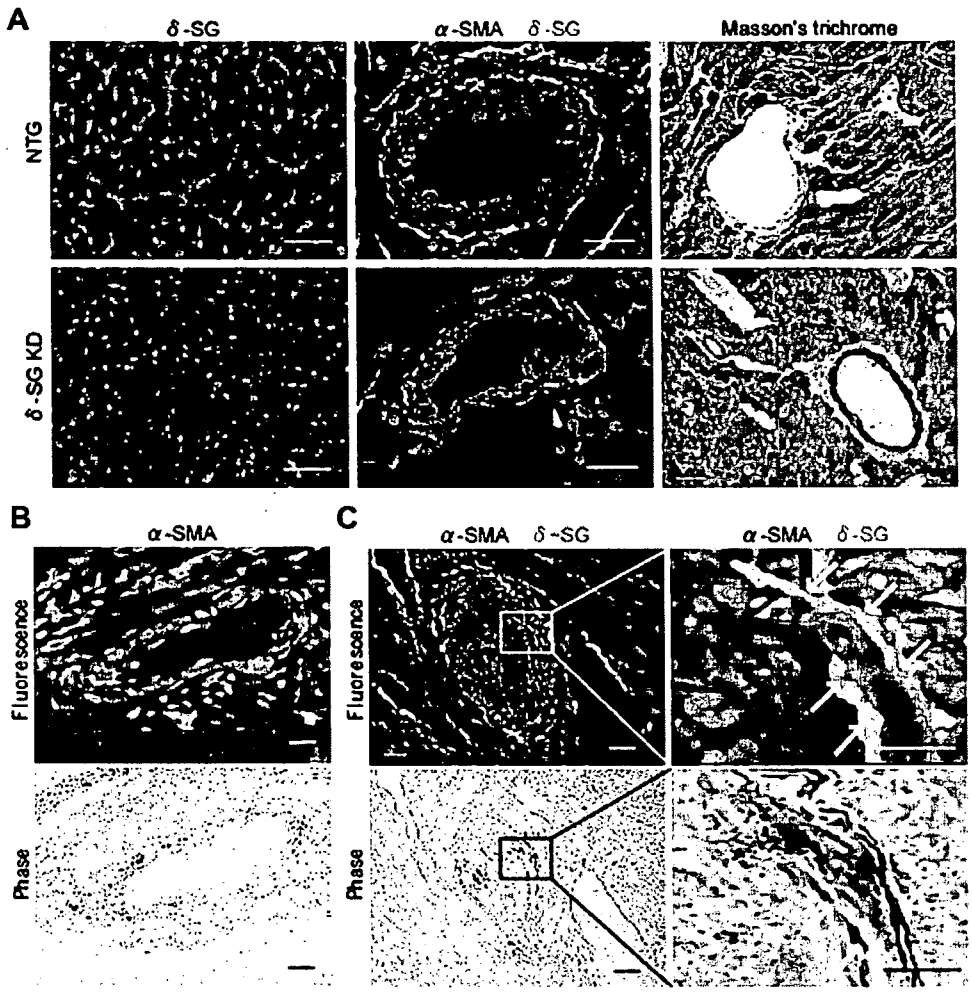

Fig. 3. Vascular regeneration in δ-SG KD hearts with the restoration of δ-SG expression. (A, left panels) Decreased δ-SG (red) expression in cardiac muscle was significantly observed in δ-SG KD hearts compared with NTG littermates. DAPI (blue). (A, middle panels) Vascular lumens were more constrictive and narrower with irregular distribution of perivascular δ-SG expression (green) in δ-SG KD hearts. α-SMA (red). DAPI (blue). (A, right panels) Masson's trichrome staining showed perivascular fibrosis in δ-SG KD hearts. (B) Transplanted LacZ$^+$ MDPCs differentiated into smooth muscle cells in δ-SG KD hearts. α-SMA (red DAPI (blue). (C) δ-SG expression (green) was restored in newly formed vessels (arrows). The right panels are magnified images of the rectangle areas in the left panels. α-SMA (red) DAPI (blue). Scale bars represent 50 μm in the left and right panels of (A), (B), and the left panels of (C), and 20 μm in the middle panels of (A) and the right panels of (C).

hearts (Fig. 4C). Transplantation of MDPCs did not result in any significant reduction in cardiac enlargement compared with that in PBS-treated hearts, but did significantly improve LV performance 4 weeks after cell implantation (Fig. 4C). To elucidate the mechanisms of functional recovery in the MDPC-transplanted hearts, relative gene expression of paracrine mediators was measured by real-time RT-PCR. Gene expression for HGF and SDF-1 significantly increased in the MDPC-implanted hearts compared with that in the control hearts 2 weeks after cell transplantation (Fig. 4D).

Discussion

Autologous transplantation is the ideal system of cell therapy. From this practical point of view, skeletal muscle is one of the most easily accessible tissue sources. There are accumulating reports of multipotent progenitors in skeletal muscle, but the differentiation potential of these cells remains controversial [2]. A recent report demonstrated the isolation of myospheres from the adult skeletal muscle [8]. As opposed to the MDPCs we described here, these cells expressed Pax7 at baseline and tended to differentiate into a myogenic lineage, suggesting that these cells were originated from satellite cells. In this study, we demonstrated Pax7$^-$ MDPCs regenerated endothelial and vascular smooth muscle cells in vitro and in vivo. These MDPCs displayed prolonged self-renewal capacity, mesenchymal cell-like phenotype, and expressed part of the embryonic stem cell markers such as Nanog, Oct-4 and Sox2 (data not shown), indicative of thier marked plasticity.

Although few reports to date have described the origin of skeletal muscle containing stem cell-like population, the characteristics of MDPCs shown here indicated that

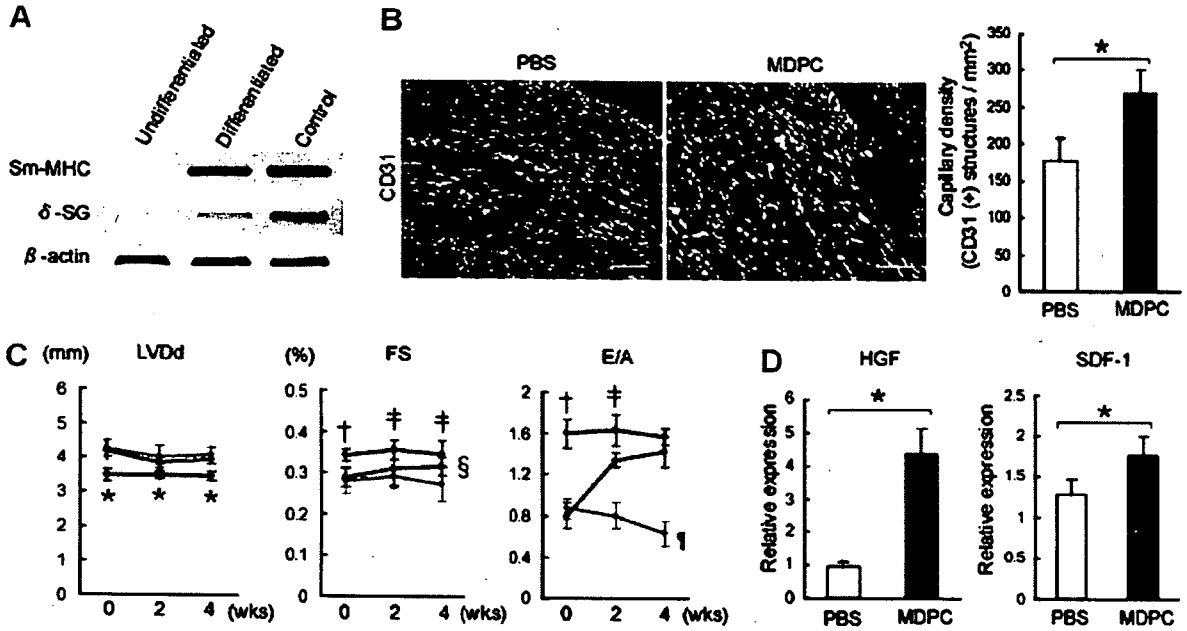

Fig. 4. MDPC transplantation improves cardiac function partially through paracrine effectors production (A) δ-SG expression was observed in differentiated MDPCs in vitro. (B) Comparison of the capillary density between PBS-treated and MDPC-transplanted δ-SG KD hearts. CD31 (red). DAPI (blue). $^{*}p < 0.01$. (C) The effect of MDPC transplantation in δ-SG KD hearts shown by echocardiograms. Black lines: NTG mice. Blue lines: PBS-treated group. Red lines: MDPC-transplanted group. $^{*}p < 0.05$; $^{\dagger}p < 0.01$ vs. PBS- and MDPC-treated mice. $^{\ddagger}p < 0.01$ vs. PBS-injected mice and $p < 0.05$ vs. MDPC-transplanted mice. $^{\S}p < 0.05$ vs. PBS-injected mice. $^{\P}p < 0.01$ vs. NTG and MDPC-treated mice compared with the same time point. (D) Relative gene expression for HGF and SDF-1 was measured by real-time RT-PCR. $^{*}p < 0.01$. Scale bars represent 50 μm in (B).

they might be reminiscent of mesenchymal cells derived from perivascular cells (PVCs) [18] or mesoangioblasts that are putative ancestors of PVCs [19], which can be classified as pericytes in capillaries and are essential for the development of functional vessel walls. Because PVCs are thought to have the potential to regenerate mesenchymal cells, MDPCs may reflect in some aspects of the phenotype of MSCs originally isolated from bone marrow stroma.

Previous report demonstrated that BM-SP cells could be engrafted in δ-SG null hearts, but failed to restore the δ-SG expression [15]. The absence of δ-SG expression after transplantation suggested that cellular fusion, as opposed to de novo differentiation, occurred with transplanted BM-SP cells which led to impaired maturation of implanted cells. In contrast, we observed that transplanted MDPCs did differentiate into mature vascular cells with the restoration of δ-SG expression, indicating autonomous vascular-differentiation might occur after MDPC transplantation.

It is important to determine whether local intramuscular injection of MDPCs into δ-SG KD heart is sufficient to deliver the cells into focally degenerated lesions and contributes to functional recovery. We observed extensive angiogenesis induced by MDPC transplantation to achieve a better preservation of cardiac function. However, the lack of improvement in diastolic dimension did not favor a scaffolding effect of the grafted MDPCs in δ-SG KD hearts similar to the previous report [20]. In our study, engrafted MDPCs were incorporated mostly into vascular cells, but muscular regeneration was rarely observed. One of the reasons is that δ-SG KD mice showed a predominantly lower expression of δ-SG along vascular smooth muscle cells, as previously reported [21], leading to scarce muscular artery and particularly extensive fibrosis surrounding the vessels. This focal defect in the δ-SG KD heart might be one of the causes for transplanted MDPCs to differentiate into vascular cells more efficiently than into cardiac or skeletal muscle fibers.

Our results also suggested that transplanted MDPCs could induce the secretion of HGF and SDF-1, that is consistent with the recent reports demonstrating that HGF could promote stem cell activation and reduced cardiomyocyte apoptosis in the myocardium of δ-SG-null hamsters [22], and that SDF-1 was sufficient to induce therapeutic stem cell homing to injured myocardium [23]. Taken together, the beneficial effects of MDPC transplantation might be due to increased blood supply produced by angiogenesis and promoted secretion of specific growth factors, leading to modulation of adverse LV remodeling and improvement of cardiac function.

In conclusion, transplantation of MDPCs induced substantial angiogenesis and increased secretion of paracrine mediators, resulting in the improvement of cardiac function in δ-SG KD mice. Our findings indicate that MDPCs may be the promising progenitor cells in adult skeletal muscle for cell therapy to treat δ-sarcoglycan complex mutant cardiomyopathy.

Acknowledgments

We thank the investigators cited for generously donating plasmids: S. Ishii, and M. Imamura; Y. Yoshida, A. Kosugi, and M. Nishikawa for technical assistance. This work was supported by Grants-in-Aid from the Ministry of Education, Culture, Sports, Science and Technology of Japan, and by Grants-in-Aid from the Ministry of Health, Labor, and Welfare of Japan.

References

[1] C.A. Collins, I. Olsen, P.S. Zammit, L. Heslop, A. Petrie, T.A. Partridge, J.E. Morgan, Stem cell function, self-renewal, and behavioral heterogeneity of cells from the adult muscle satellite cell niche, Cell 122 (2005) 289–301.

[2] I.W. McKinnell, G. Parise, M.A. Rudnicki, Muscle stem cells and regenerative myogenesis, Curr. Top Dev. Biol. 71 (2005) 113–130.

[3] N. Hashimoto, T. Murase, S. Kondo, A. Okuda, M. Inagawa-Ogashiwa, Muscle reconstitution by muscle satellite cell descendants with stem cell-like properties, Development 131 (2004) 5481–5490.

[4] Z. Qu-Petersen, B. Deasy, R. Jankowski, M. Ikezawa, J. Cummins, R. Pruchnic, J. Mytinger, B. Cao, C. Gates, A. Wernig, J. Huard, Identification of a novel population of muscle stem cells in mice: potential for muscle regeneration, J. Cell Biol. 157 (2002) 851–864.

[5] H. Oshima, T.R. Payne, K.L. Urish, T. Sakai, Y. Ling, B. Gharaibeh, K. Tobita, B.B. Keller, J.H. Cummins, J. Huard, Differential myocardial infarct repair with muscle stem cells compared to myoblasts, Mol. Ther. 12 (2005) 1130–1141.

[6] T.R. Payne, H. Oshima, T. Sakai, Y. Ling, B. Gharaibeh, J. Cummins, J. Huard, Regeneration of dystrophin-expressing myocytes in the mdx heart by skeletal muscle stem cells, Gene Ther. 12 (2005) 1264–1274.

[7] T. Tamaki, A. Akatsuka, K. Ando, Y. Nakamura, H. Matsuzawa, T. Hotta, R.R. Roy, V.R. Edgerton, Identification of myogenic-endothelial progenitor cells in the interstitial spaces of skeletal muscle, J. Cell Biol. 157 (2002) 571–577.

[8] R. Sarig, Z. Baruchi, O. Fuchs, U. Nudel, D. Yaffe, Regeneration and transdifferentiation potential of muscle-derived stem cells propagated as myospheres, Stem Cells 24 (2006) 1769–1778.

[9] H. Gerhardt, C. Betsholtz, Endothelial-pericyte interactions in angiogenesis, Cell Tissue Res. 314 (2003) 15–23.

[10] L. da Silva Meirelles, P.C. Chagastelles, N.B. Nardi, Mesenchymal stem cells reside in virtually all post-natal organs and tissues, J. Cell Sci. 119 (2006) 2204–2213.

[11] M.F. Pittenger, B.J. Martin, Mesenchymal stem cells and their potential as cardiac therapeutics, Circ. Res. 95 (2004) 9–20.

[12] A. Sakamoto, K. Ono, M. Abe, G. Jasmin, T. Eki, Y. Murakami, T. Masaki, T. Toyo-oka, F. Hanaoka, Both hypertrophic and dilated cardiomyopathies are caused by mutation of the same gene, delta-sarcoglycan, in hamster: an animal model of disrupted dystrophin-associated glycoprotein complex, Proc. Natl. Acad. Sci. USA 94 (1997) 13873–13878.

[13] R. Coral-Vazquez, R.D. Cohn, S.A. Moore, J.A. Hill, R.M. Weiss, R.L. Davisson, V. Straub, R. Barresi, D. Bansal, R.F. Hrstka, R. Williamson, K.P. Campbell, Disruption of the sarcoglycan-sarcospan complex in vascular smooth muscle: a novel mechanism for cardiomyopathy and muscular dystrophy, Cell 98 (1999) 465–474.

[14] T. Shinagawa, S. Ishii, Generation of Ski-knockdown mice by expressing a long double-strand RNA from an RNA polymerase II promoter, Genes Dev. 17 (2003) 1340–1345.

[15] K.A. Lapidos, Y.E. Chen, J.U. Earley, A. Heydemann, J.M. Huber, M. Chien, A. Ma, E.M. McNally, Transplanted hematopoietic stem cells demonstrate impaired sarcoglycan expression after engraftment into cardiac and skeletal muscle, J. Clin. Invest. 114 (2004) 1577–1585.

[16] S. Noguchi, E. Wakabayashi, M. Imamura, M. Yoshida, E. Ozawa, Developmental expression of sarcoglycan gene products in cultured myocytes, Biochem. Biophys. Res. Commun. 262 (1999) 88–93.

[17] P. Vourc'h, M. Romero-Ramos, O. Chivatakarn, H.E. Young, P.A. Lucas, M. El-Kalay, M.F. Chesselet, Isolation and characterization of cells with neurogenic potential from adult skeletal muscle, Biochem. Biophys. Res. Commun. 317 (2004) 893–901.

[18] B. Brachvogel, H. Moch, F. Pausch, U. Schlotzer-Schrehardt, C. Hofmann, R. Hallmann, K. von der Mark, T. Winkler, E. Poschl, Perivascular cells expressing annexin A5 define a novel mesenchymal stem cell-like population with the capacity to differentiate into multiple mesenchymal lineages, Development 132 (2005) 2657–2668.

[19] G. Cossu, P. Bianco, Mesoangioblasts—vascular progenitors for extravascular mesodermal tissues, Curr. Opin. Genet. Dev. 13 (2003) 537–542.

[20] J. Pouly, A.A. Hagege, J.T. Vilquin, A. Bissery, A. Rouche, P. Bruneval, D. Duboc, M. Desnos, M. Fiszman, Y. Fromes, P. Menasche, Does the functional efficacy of skeletal myoblast transplantation extend to nonischemic cardiomyopathy? Circulation 110 (2004) 1626–1631.

[21] M.T. Wheeler, M.J. Allikian, A. Heydemann, M. Hadhazy, S. Zarnegar, E.M. McNally, Smooth muscle cell-extrinsic vascular spasm arises from cardiomyocyte degeneration in sarcoglycan-deficient cardiomyopathy, J. Clin. Invest. 113 (2004) 668–675.

[22] R. Fiaccavento, F. Carotenuto, M. Minieri, C. Fantini, G. Forte, A. Carbone, L. Carosella, R. Bei, L. Masuelli, C. Palumbo, A. Modesti, M. Prat, P. Di Nardo, Stem cell activation sustains hereditary hypertrophy in hamster cardiomyopathy, J. Pathol. 205 (2005) 397–407.

[23] A.T. Askari, S. Unzek, Z.B. Popovic, C.K. Goldman, F. Forudi, M. Kiedrowski, A. Rovner, S.G. Ellis, J.D. Thomas, P.E. DiCorleto, E.J. Topol, M.S. Penn, Effect of stromal-cell-derived factor 1 on stem-cell homing and tissue regeneration in ischaemic cardiomyopathy, Lancet 362 (2003) 697–703.

Available online at www.sciencedirect.com
ScienceDirect
ELSEVIER
Biochemical and Biophysical Research Communications 350 (2006) 1006–1012
BBRC
www.elsevier.com/locate/ybbrc

MicroRNA-1 facilitates skeletal myogenic differentiation without affecting osteoblastic and adipogenic differentiation

Norio Nakajima [a,b], Tomosaburo Takahashi [a,b,*], Ryoji Kitamura [a,b], Koji Isodono [a,b], Satoshi Asada [a,b], Tomomi Ueyama [b], Hiroaki Matsubara [a,b], Hidemasa Oh [b]

[a] *Department of Cardiovascular Medicine, Kyoto Prefectural University of Medicine, Kyoto 602-8566, Japan*
[b] *Department of Experimental Therapeutics, Translational Research Center, Kyoto University Hospital, Kyoto 606-8507, Japan*

Received 26 September 2006
Available online 6 October 2006

Abstract

MicroRNAs (miRNAs) are small non-coding RNAs emerging as important post-transcriptional gene regulators. In this study, we examined the role of miR-1, an miRNA specifically expressed in cardiac and skeletal muscle tissue, on the myogenic, osteoblastic, and adipogenic differentiation of C2C12 cells. Upon induction of myogenic differentiation, miR-1 was robustly expressed. Retrovirus-mediated overexpression of miR-1 markedly enhanced expression of muscle creatine kinase, sarcomeric myosin, and α-actinin, while the effects on myogenin and MyoD expression were modest. Formation of myotubes was significantly augmented in miR-1-overexpressing cells, indicating miR-1 expression enhanced not only myogenic differentiation but also maturation into myotubes. In contrast, osteoblastic and adipogenic differentiation was not affected by forced expression of miR-1. Thus, the muscle-specific miRNA, miR-1, plays important roles in controlling myogenic differentiation and maturation in lineage-committed cells, rather than functioning in fate determination.

Keywords: MicroRNA; Differentiation; Skeletal muscle cells; Adipocytes; Osteoblasts; C2C12 cells

MicroRNAs (miRNAs) are a class of small non-coding RNAs that play an important role in the post-transcriptional regulation of protein-coding gene expression. They anneal to the complementary sequences in the 3'UTRs of target mRNAs and cause degradation or, more notably, translational inhibition of target transcripts [1]. Although the functions of only a handful of miRNAs have been identified, it is emerging that miRNAs are involved in a wide variety of biological functions such as developmental patterning, lineage differentiation, cell death, proliferation, insulin secretion, and antiviral defense [2]. MiRNA-1 (miR-1) is an miRNA that is specifically expressed in cardiac and skeletal muscle [3]. Transfection of miR-1 in HeLa cells, a human epithelial cell line, has been shown to shift the gene expression profile toward that of muscle cells [4]. It has also been shown that transgenic expression of miR-1 in mouse hearts results in a proliferation defect and a failure of cardiac myocyte expansion, suggesting premature differentiation of cardiac myocytes by miR-1 overexpression [3]. A recent study revealed that miR-1 promotes myogenesis of myoblasts while repressing proliferation [5], although only relatively early steps of myoblast differentiation were examined in this study. These studies suggest that miR-1 regulates the balance between differentiation and proliferation, but the roles of miR-1 in lineage specification and terminal differentiation remain to be clarified.

The C2C12 cell line is a subclone isolated from parental C2 cells established from the regenerating thigh muscle of an adult mouse. Although C2C12 cells are widely used as a myoblast cell line, these cells are also well characterized as mesenchymal progenitor cells, and can differentiate into several mesenchymal cell types including myocytes,

* Corresponding author. Fax: +81 75 251 5514.
E-mail address: ttaka@koto.kpu-m.ac.jp (T. Takahashi).

0006-291X/$ - see front matter © 2006 Elsevier Inc. All rights reserved.
doi:10.1016/j.bbrc.2006.09.153

osteoblasts, and adipocytes [6,7]. Incubation of C2C12 cells under low serum conditions induces muscle differentiation and fusion of cells into multinucleated myotubes. Treatment of C2C12 cells with bone morphogenetic protein (BMP)-2 blocks myotube formation and induces osteogenic differentiation instead [6,8,9]. Culturing the cells with adipogenic medium, treatment with long-chain fatty acids, or treatment with thiazolidinediones also blocks myotube formation and leads to typical adipocyte differentiation [7,10]. During differentiation into these cell types, the cells capture important aspects of their respective differentiation programs such as expression of tissue-specific transcription factors and functional gene products, providing unique opportunities to study the mechanisms of differentiation into these mesenchymal cell types.

Understanding the molecular mechanisms that control differentiation into various specialized types of cells is crucial not only for the advancement of stem or progenitor cell biology, but also for developing its clinical potential as a tissue regeneration therapy. Formation of specialized cells is a multistep process of specific cellular events that includes commitment into specific lineages, differentiation, and maturation. In this study, we used C2C12 cell differentiation as a model system to determine whether miR-1 plays a role in myogenic, osteoblastic, and adipogenic differentiation.

Materials and methods

Cell culture and differentiation induction. C2C12 cells (a kind gift from A. Takahashi) and 3T3-L1 cells (Japanese Collection of Research Bioresources) were maintained as described previously [11,12]. Myogenesis was induced by changing the growth medium to DMEM supplemented with 2% horse serum after the cells reached confluency [11]. Osteoblastic differentiation was induced by treating cells with 300 ng/ml recombinant human BMP-2 (Astellas Pharma) [13]. For adipogenic differentiation, the growth medium was switched to adipogenic induction medium for 3 days and subsequently to adipogenic maintenance medium for 7 days as described previously [10].

Northern blot analysis. Total RNA samples extracted using TRIZOL (Invitrogen) were electrophoresed on denaturing 15% polyacrylamide gels and electroblotted onto GeneScreen Plus membranes (Perkin-Elmer). The membranes were UV-crosslinked, baked, and hybridized with ^{32}P end-labeled oligonucleotide DNA probes in ULTRAhyb-Oligo (Ambion). After washing, hybridization signals were detected using the Bio-imaging analyzer system BAS5000 (Fuji Film). Mouse U6 was used as an internal control.

Immunofluorescent microscopy and quantitative analyses of myotubes. Cells were stained with an antibody against sarcomeric myosin (MF20; Developmental Studies Hybridoma Bank) followed by Alexa Fluor 555-conjugated anti-mouse IgG antibody (Invitrogen) with nuclear staining with DAPI. The average number of nuclei per myotube was determined by counting randomly chosen myosin-positive cells containing two or more nuclei, and 1000 nuclei per culture were counted. The fusion index was calculated as the ratio of the number of nuclei in myotubes with two or more nuclei to the total number of nuclei, and 5000 myotube nuclei were counted.

Oil red O staining and alkaline phosphatase (ALP) assays. Cells were fixed and stained with Oil Red O solution as described previously [12]. Oil Red O was eluted with 100% 2-propanol and measured at 490 nm absorbance for quantification. For ALP staining, cells were stained with a mixture of 0.01% (w/v) naphthol AS-MX phosphate and 0.25 mg/ml fast violet B salt (Sigma–Aldrich) and counterstained with Mayer's Hematoxylin Solution. ALP activity was determined with *p*-nitrophenyl phosphate as a substrate.

DNA constructs. To express miR-1 under the control of the U6 promoter, miR-1 precursor sequences were synthesized, annealed, and ligated into the pENTR/U6 vector (Invitrogen). An miR-1 expression plasmid under the control of the long terminal repeat of PCMV virus was constructed using genomic sequences of miR1-2 containing pre-miR-1 gene sequences with 50 bp flanking each side, and the pMSCV-puro vector (Clontech). For use as a control, a pMSCV-puro vector expressing EGFP was also made.

Retrovirus production and infection. GP2-293 cells were cotransfected with the envelop vector pVSV-G and pMSCV-puro vectors using FuGENE6 (Roche). The medium supernatant was collected and centrifuged to concentrate virus stocks according to the manufacturer's instruction. Cells were infected with the retrovirus in the presence of 4 μg/ml polybrene for 24 h, and the infected cells were selected with 2.5 μg/ml puromycin.

Reverse transcriptase (RT)-polymerase chain reaction (PCR). cDNA was synthesized and analyzed by kinetic real-time PCR using the ABI Prism 7700 Sequence Detector system (Applied Biosystems) with Platinum SYBR Green qPCR SuperMix (Invitrogen). Mouse β tubulin was used for normalization, and comparative threshold (C_T) method was used to assess relative abundance of the targets. Primers used were myogenin-f: TACGT CCATCGTGGACAGCAT, myogenin-r: TCAGCTAAATTCCCT CGCTGG; myoD-f: ACATAGACTTGACAGGCCCCGA, myoD-r: AGACCTTCGATGTAGCGGATGG; muscle creatine kinase (MCK)-f: CACCTCCACAGCACAGACAG, MCK-r: ACCTTGGCCATGTGAT TGTT; β-tubulin-f: GGAACATAGCCGTAAACTGC, β-tubulin-r: TCA CTGTGCCTGAACTTACC; osterix-f: GGGTTAAGGGGAGCAAAG TCAGAT, osterix-r: CTGGGGAAAGGAGGCACAAAGAAG; osteocalcin-f: CTGAGTCTGACAAAGCCTTC, osteocalcin-r: GCTGTGAC ATCCATACTTGC; ALP-f: AACCCAGACACAAGCATTCC, ALP-r: GCCTTTGAGGTTTTTGGTCA; PPARγ-f: CCCTGGCAAAGCA TTTGTAT, PPARγ-r: GAAACTGGCACCCTTGAAAA; C/EBPα-f: GAACAGCAACGAGTACCGGGTA, C/EBPα-r: GCCATGGCCTTG ACCAAGGAG; aP2-f: CCGCAGACGACAGGA, aP2-r: CTCATGC CCTTTCATAAACT.

Immunoblot analysis. Cell lysates containing equal amounts of protein were electrophoresed on 10% SDS–polyacrylamide gels and transferred to polyvinylidene difluoride membranes (Millipore). Blots were immunoblotted with the primary antibody against sarcomeric myosin, α-actinin (EA-53; Sigma–Aldrich) or α-tubulin (Sigma–Aldrich), and horseradish peroxidase-labeled donkey anti-mouse IgG as a secondary antibody, followed by enhanced chemiluminescence (GE Healthcare) [14].

Statistical analysis. All experiments were performed at least three times. Data were expressed as means ± standard error and analyzed by one-way ANOVA with post hoc analysis. A value of $P < 0.05$ was considered statistically significant.

Results and discussion

MiR-1 is a muscle-specific miRNA that is expressed during myogenic differentiation

We first examined the expression of miR-1 in C2C12 cells during differentiation into myocytes, osteoblasts, and adipocytes. Although myotube formation was completely abolished when cells were induced to differentiate into osteoblasts, myotube formation was evident upon adipogenic differentiation (Fig. 1A). In undifferentiated cells, miR-1 was not expressed, while its expression was robustly increased when cells were induced to differentiate into myotubes, but not into osteoblasts (Fig. 1B). MiR-1 expression was also observed upon adipogenic differentiation, which

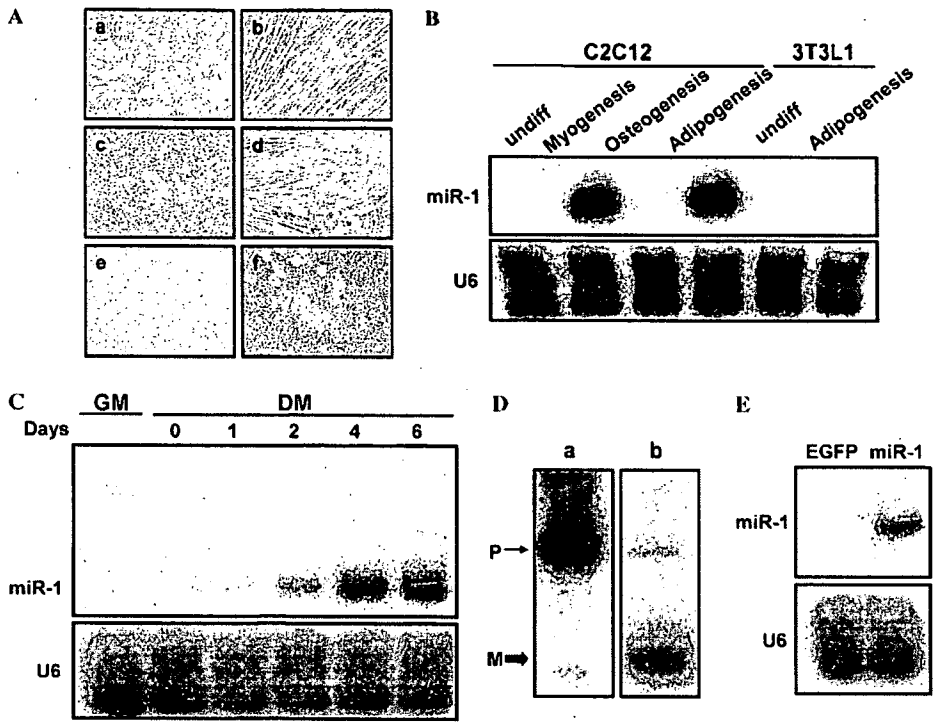

Fig. 1. MiR-1 is a muscle-specific miRNA that is expressed during myogenic differentiation. (A) Myogenic, osteoblastic, and adipogenic differentiation was induced in C2C12 cells (a–d) and 3T3-L1 cells (e,f). (a,e) Undifferentiated, (b) myogenic differentiation, (c) osteogenic differentiation, (d,f) adipogenic differentiation. (B) MiR-1 expression was analyzed in C2C12 cells or 3T3-L1 cells treated as indicated. (C) Myogenic differentiation was induced in C2C12 cells for the indicated periods of time (DM) or cells were cultured in growth medium (GM). Northern blot analysis was performed for miR-1 expression. (D) 293 cells were transfected with the pre-miR-1 (a) or the pri-miR-1-like molecule (b) expression vector, and miR-1 expression was analyzed. P, pre-miR-1; M, mature miR-1. (E) C2C12 cells were infected with EGFP or miR-1-expressing retrovirus vector, and miR-1 expression was analyzed. U6 was used as a loading control.

might reflect concomitant differentiation into myotubes in the adipogenic condition used in this study (Fig. 1A and B). MiR-1 expression was not observed in adipogenic differentiation of 3T3-L1 pre-adipocytes, where myotube formation was not observed (Fig. 1A and B). The observation that miR-1 expression was restricted to conditions that induced myotube formation was consistent with the previously observed restriction of miR-1 expression to cardiac and skeletal muscle in adult mice [3]. Kinetic analysis of miR-1 expression in myogenic differentiation revealed that miR-1 expression was readily detectable 2 days after induction of differentiation and reached its maximum at around days 4–6 (Fig. 1C). This time course correlated well with the expression of myogenic markers such as myogenin, a myogenic regulatory factor (MRF), and muscle type creatine kinase (MCK), a well-characterized marker for mature myocytes (Fig. 2), suggesting that miR-1 plays a role in controlling myogenic differentiation programs.

Overexpression of miR-1 facilitates myogenic differentiation

To analyze the role of miR-1 in C2C12 cell differentiation, we developed a vector-based expression system which efficiently expressed exogenous mature miR-1 in cells, since transient expression by synthetic RNA molecule transfection is not suitable for stable expression during the time course of C2C12 cell differentiation. When a precursor of miR-1 (pre-miR-1) was expressed under the control of the RNA polymerase III promoter, processing from the precursor to mature miR-1 was largely impaired, as revealed by much less abundance of mature miR-1 than pre-miR-1 (Fig. 1D). We then expressed a primary miR-1 (pri-miR-1) like molecule, consisting of the pre-miR-1 plus an additional 50 nucleotides taken from its genomic sequence on each end, under the control of the RNA polymerase II promoter. With this system, efficient expression of mature miR-1 was achieved (Fig. 1D), indicating that exogenous expression of pre-miR-1 is not sufficient for entering the proper processing mechanism, whereas expression of a pri-miR1-like molecule facilitates mature miR-1 expression. Therefore, we made a retroviral vector with this construct for efficient production of mature miR-1 in C2C12 cells (Fig. 1E).

Myogenic differentiation is a multistep dynamic process, during which the cells are defined to be myogenic (terminal commitment), differentiate into myocytes expressing muscle-specific structural and enzymatic proteins (biochemical differentiation), and subsequently fuse to form mature multinucleated myotubes (terminal differentiation). Progression through myogenic differentiation is controlled by

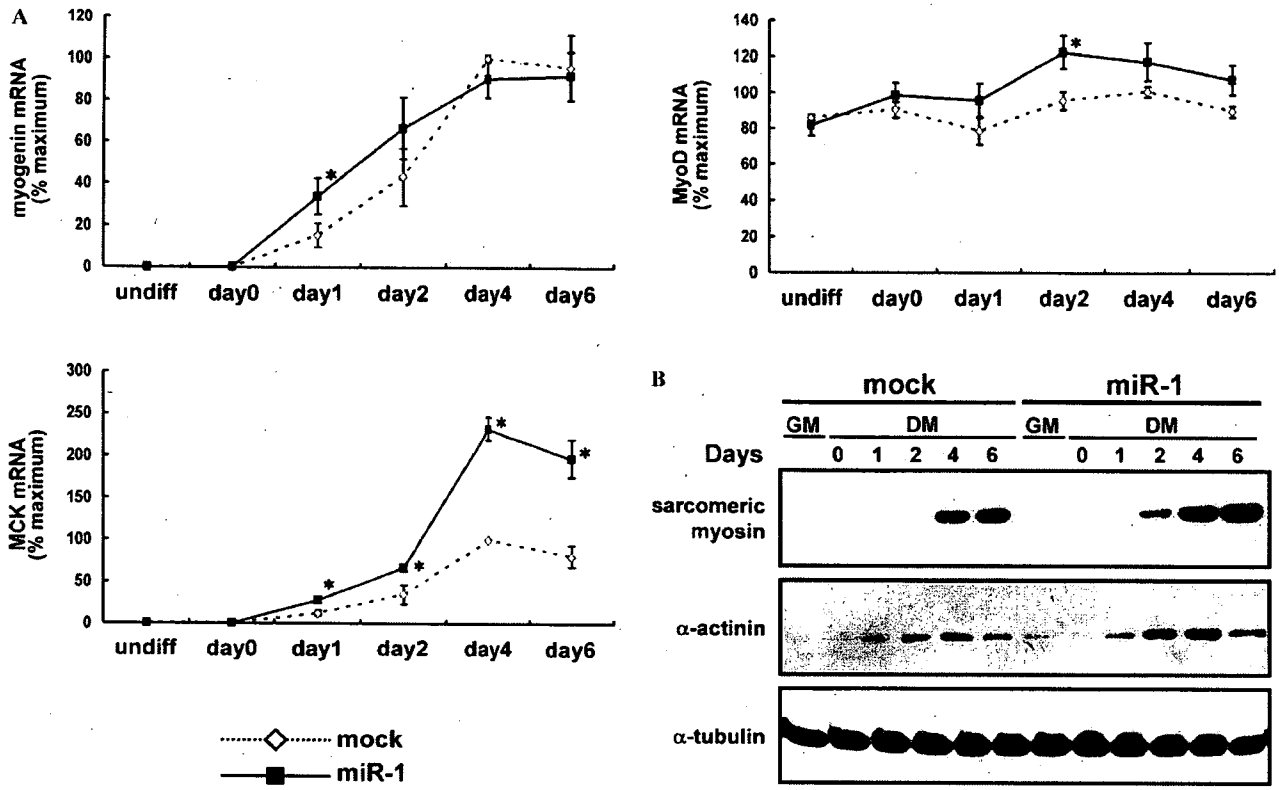

Fig. 2. Overexpression of miR-1 facilitates myogenic differentiation. Myogenic differentiation was induced for the indicated periods of time in C2C12 cells infected with mock or miR-1-expressing retrovirus. (A) Myogenin, MyoD, and MCK expression was analyzed with kinetic real-time PCR. The results were expressed as relative expression to β-tubulin and plotted as percentages of the maximum levels seen in mock-infected cells. $^*P < 0.05$ versus control. (B) Immunoblot analysis was performed using anti-sarcomeric myosin, anti-sarcomeric α-actinin, and anti-α-tubulin antibodies.

sequential activation of members of muscle-specific basic helix-loop-helix proteins called MRFs [15]. Among them, MyoD is expressed in undifferentiated myoblasts, while myogenin is activated during differentiation into myocytes. Myogenin expression in miR-1-overexpressing cells was accelerated at day 1, exhibiting a 2.1-fold increase in miR-1-overexpressing cells over mock-infected cells (Fig. 2A). A recent study [5] reported a similar observation, where the effect of transfection of a synthetic miR-1 duplex on myogenin expression was evaluated up to 24 h after induction of differentiation. Later time points were then examined with the aid of retrovirus-mediated stable expression of miR-1. Myogenin expression was comparable between miR-1-overexpressing cells and control cells after day 4, and a modest increase in MyoD expression was observed by miR-1 overexpression only in the differentiating state (Fig. 2A). However, a striking increase was observed in MCK expression in miR-1-overexpressing cells compared to mock-infected cells in the late phase (Fig. 2A). About a 2.7- and 3.8-fold enhancement in MCK expression in miR-1 cells was observed at day 4 and 6, respectively. Western blot analysis with anti-sarcomeric myosin and anti-sarcomeric α-actinin antibodies revealed that expression of these structural proteins was not only accelerated but also augmented by miR-1 overexpression (Fig. 2B). These results indicated that miR-1 overexpression enhanced the biochemical differentiation of myocytes.

MiR-1 overexpression leads to enhanced formation of multinucleated mature myotubes

Fusion of individual myocytes to form multinucleated mature myotubes is a unique feature of skeletal myogenic differentiation, and myoblast fusion has been shown to be regulated by mechanisms genetically dissociated from other myogenic processes such as biochemical differentiation [16–19]. Therefore, we analyzed the effect of miR-1 expression on the formation of mature myotubes and observed that in miR-1-overexpressing cells, myotubes were both higher in number and larger in size compared to mock-infected cells (Fig. 3A). This observation was quantified by the average number of nuclei per myotube (Fig. 3B), and by the percentage of all nuclei present in myotubes (fusion index) [20] (Fig. 3C). The results showed about a 1.9-fold increase in nuclei per myotube and a 1.6-fold increase in the fusion index.

Taken together, these results indicate that in addition to its role in the early steps of myogenic differentiation [5], miR-1 also plays an important role in late biochemical differentiation and in terminal differentiation. This was

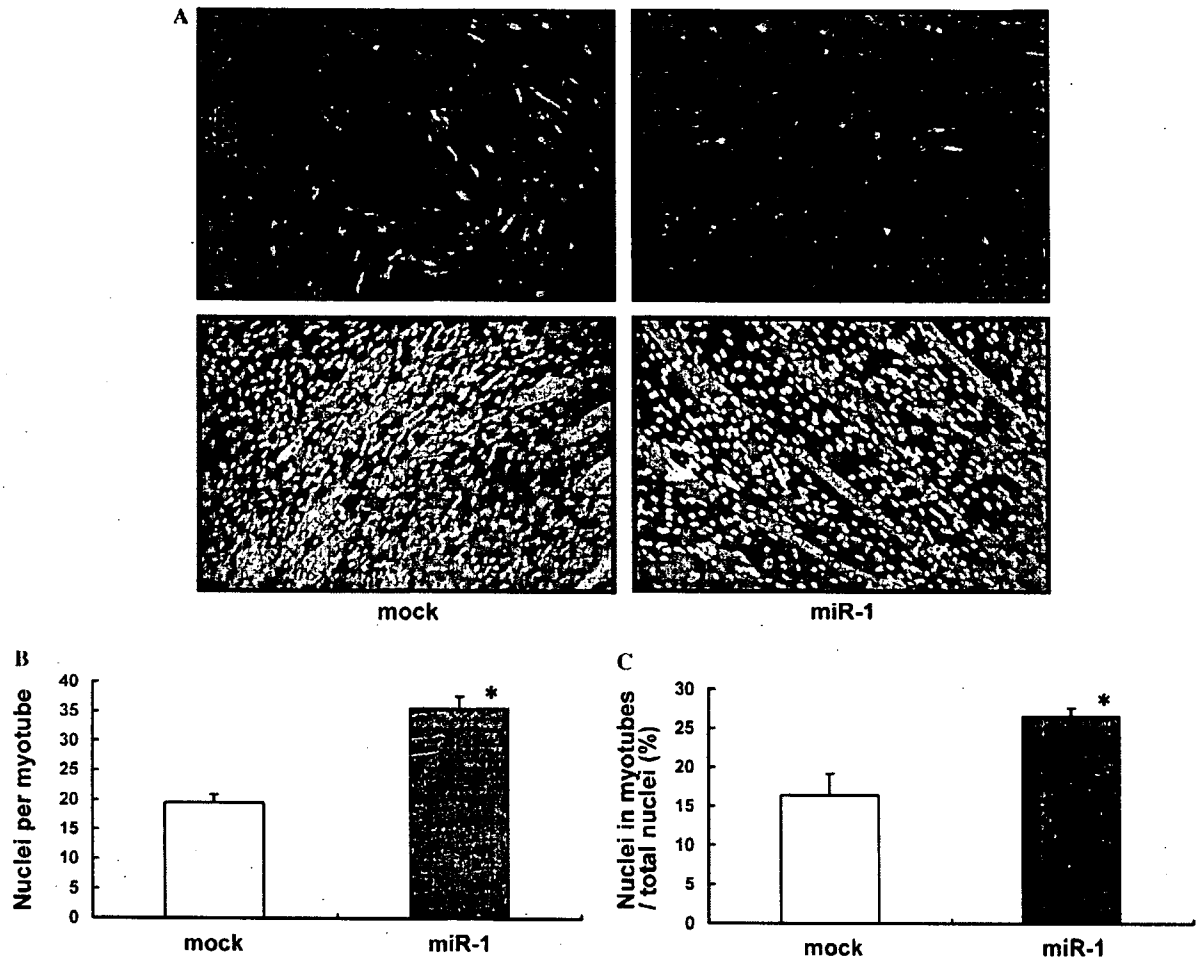

Fig. 3. MiR-1 overexpression leads to enhanced formation of multinucleated mature myotubes. Cells infected with mock or miR-1-expressing retrovirus were induced for myogenic differentiation for 6 days. (A) Myotubes were stained with anti-sarcomeric myosin antibody, and nuclei were stained with DAPI. (B) The mean number of nuclei per myotube was determined by counting 1000 nuclei per culture in three independent cultures. (C) The fusion index was defined as the ratio of nuclei within myotubes (cells containing two or more nuclei) to total number of nuclei, and percentages were plotted. Five thousand nuclei per culture were counted in three independent cultures. $^*P < 0.05$ versus control.

supported by: (i) the similar kinetics of endogenous miR-1 expression (Fig. 1C) with the expression of MCK, sarcomeric myosin, and α-actinin (Fig. 2A and B), and the formation of myotubes, which all peaked at days 4–6 after induction; and (ii) the enhancement of expression of mature myocyte markers and myotube fusion with overexpression of miR-1.

In the heart, which also endogenously expresses miR-1, it has been reported that overexpression of miR-1 in mouse hearts leads to a decrease in proliferating ventricular cardiac myocytes [3]. Although the role of miR-1 in the determination of myocyte fate could not be evaluated in this study, as a cardiac-specific β-myosin heavy chain promoter was used to drive miR-1 expression in cardiac myocytes, these results suggest that miR-1 expression in cardiac myocytes results in enhanced or premature differentiation of cardiac myocytes that impairs the balance between differentiation and proliferation. CHIP assays have demonstrated that MyoD and myogenin bind to regions upstream to miR-1 genes, suggesting these MRFs regulate expression of miR-1 [21]. These results with our observations suggested that miR-1 plays an important role in the relatively late stages of myogenic differentiation, although further studies are needed to fully clarify the functions of miR-1 in myogenesis.

MiR-1 does not influence osteoblastic or adipogenic differentiation

Since it is not known whether miR-1 plays a role in specification of cell fate to myogenic lineages, we analyzed the effects of miR-1 overexpression on the osteoblastic and adipogenic differentiation of C2C12 cells. The osteoblastic and adipogenic differentiation programs are also multistep processes [10,12,22,23], so we evaluated the expression of transcription factors involved in determination and initial differentiation of these lineages such as osterix, PPARγ, and C/EBPα, relatively late differentiation markers such

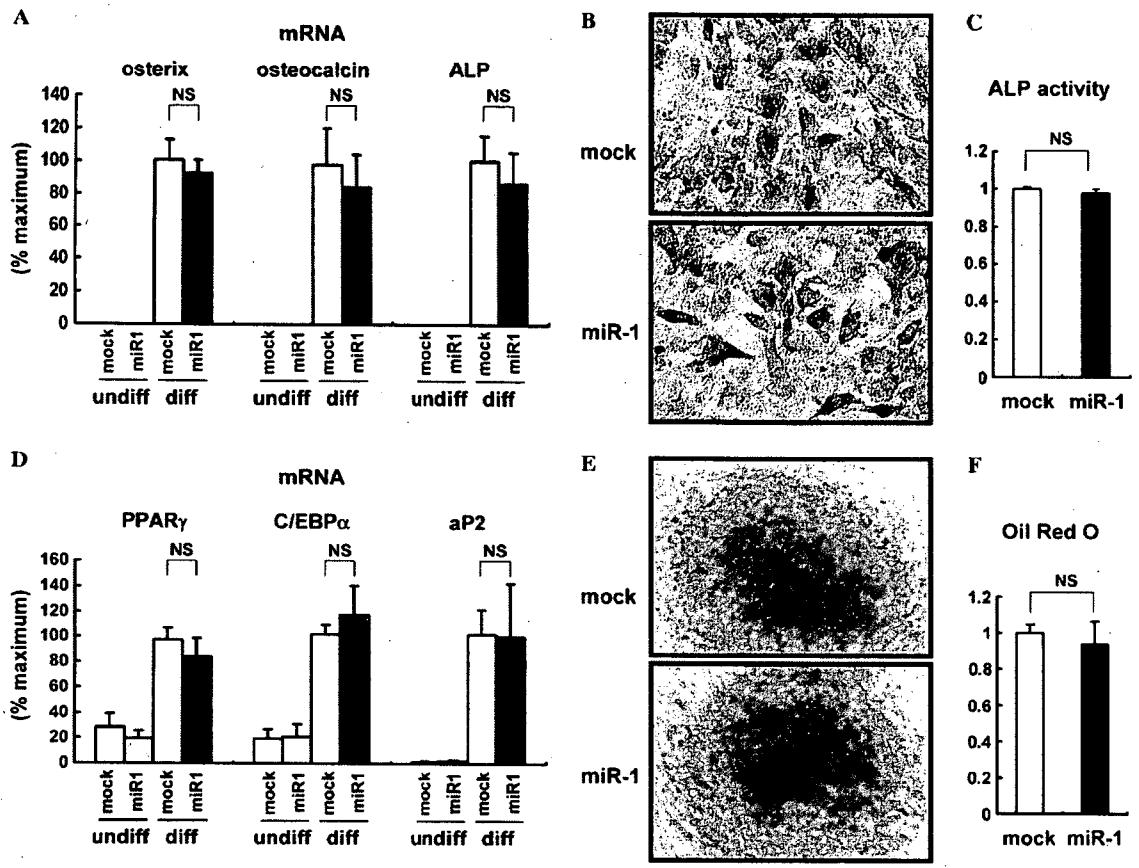

Fig. 4. MiR-1 does not influence osteoblastic or adipogenic differentiation. Osteoblastic (A–C) or adipogenic (D–F) differentiation was induced in mock-infected and miR-1-overexpressing C2C12 cells. (A) Osterix, osteocalcin, and ALP expression was measured by kinetic real-time PCR in undifferentiated and differentiated cells. (B) ALP staining was performed in differentiated cells. (C) ALP activity was determined with *p*-nitrophenyl phosphate as a substrate. (D) Kinetic PCR analysis was performed to analyze expression of PPARγ, C/EBPα, and aP2 in undifferentiated and differentiated cells. (E) Differentiated cells were stained with Oil Red O. (F) To quantify lipid accumulation, Oil Red O was extracted, and optical density was measured at 490 nm. NS; not significant.

as osteocalcin, ALP, and aP2, and characteristic biochemical features of these cells such as ALP activity and lipid accumulation. The osteoblastic markers osterix, osteocalcin, and ALP were absent in undifferentiated C2C12 cells, but markedly induced upon induction of osteoblastic differentiation (Fig. 4A). Neither the expression of these osteoblastic markers nor ALP staining and activity was altered by the exogenous expression of miR-1 during osteoblastic differentiation (Fig. 4A–C). When cells were cultured in adipogenic condition, adipogenic markers such as PPARγ, C/EBPα, and aP2 and lipid accumulation were significantly induced, and the forced expression of miR-1 did not alter the expression of these adipogenic marker genes or lipid accumulation in the cells (Fig. 4D–F). It has been reported that exogenous miR-1 expression in non-muscle cells shifts the mRNA expression profile towards muscle by downregulating the expression of genes not expressed in muscle [4]. Although these results suggested that miR-1 might act to prevent cells from differentiating into lineages other than muscle, our results showed that osteoblastic and adipogenic differentiation was not modulated by the expression of miR-1, implying that miR-1 does not function in determination of cell fate.

Conclusion

In this study, we analyzed the role of miR-1 in myogenic, osteoblastic, and adipogenic differentiation of C2C12 cells, and found that miR-1 enhanced myogenic differentiation and maturation into myotubes, but did not affect osteoblastic and adipogenic differentiation. These results suggest that miR-1 plays important roles in controlling the myogenic differentiation and maturation in lineage-committed cells, rather than functioning in fate determination. Identification of downstream targets of miR-1 will be an important issue to fully clarify the roles of miR-1 in myogenesis, which could be coordinately regulated by multiple miR-1 targets, since bioinformatic predictions indicate that each miRNA regulates on average ~200 target transcripts [24].

Acknowledgments

We thank Akihiro Takahashi for providing C2C12 cells, Astellas Pharma for BMP-2, Parth Patwari for critical reading of the manuscript, and Atsumi Kosugi and Mami Nishikawa for expert technical assistance. This work was supported by Grants-in-Aid from the Ministry of Education, Culture, Sports, Science and Technology of Japan, a grant from the Mitsubishi Pharma Research Foundation and Grants-in-Aid from the Ministry of Health, Labor, and Welfare of Japan.

References

[1] P.H. Olsen, V. Ambros, The *lin-4* regulatory RNA controls developmental timing in *Caenorhabditis elegans* by blocking LIN-14 protein synthesis after the initiation of translation, Dev. Biol. 216 (1999) 671–680.

[2] E. Wienholds, R.H.A. Plasterk, MicroRNA function in animal development, FEBS Lett. 579 (2005) 5911–5922.

[3] Y. Zhao, E. Samal, D. Srivastava, Serum response factor regulates a muscle-specific microRNA that targets *Hand2* during cardiogenesis, Nature 436 (2005) 214–220.

[4] L.P. Lim, N.C. Lau, P. Garrett-Engele, A. Grimson, J.M. Schelter, J. Castle, D.P. Bartel, P.S. Linsley, J.M. Johnson, Microarray analysis shows that some microRNAs downregulate large numbers of target mRNAs, Nature 433 (2005) 769–773.

[5] J.F. Chen, E.M. Mandel, J.M. Thomson, Q. Wu, T.E. Callis, S.M. Hammond, F.L. Conlon, D.Z. Wang, The role of microRNA-1 and microRNA-133 in skeletal muscle proliferation and differentiation, Nat. Genet. 38 (2006) 228–233.

[6] \T. Katagiri, A. Yamaguchi, M. Komaki, E. Abe, N. Takahashi, T. Ikeda, V. Rosen, J.M. Wozney, A. Fujisawa-Sehara, T. Suda, Bone morphogenetic protein-2 converts the differentiation pathway of C2C12 myoblasts into the osteoblast lineage, J. Cell Biol. 127 (1994) 1755–1766.

[7] L. Teboul, D. Gaillard, L. Staccini, H. Inadera, E.Z. Amri, P.A. Grimaldi, Thiazolidinediones and fatty acids convert myogenic cells into adipose-like cells, J. Biol. Chem. 270 (1995) 28183–28187.

[8] E. Chalaux, T. Lopez-Rovira, J.L. Rosa, R. Bartrons, F. Ventura, JunB is involved in the inhibition of myogenic differentiation by bone morphogenetic protein-2, J. Biol. Chem. 273 (1998) 537–543.

[9] D.S. de Jong, W.T. Steegenga, J.M. Hendriks, E.J. van Zoelen, W. Olijve, K.J. Dechering, Regulation of Notch signaling genes during BMP2-induced differentiation of osteoblast precursor cells, Biochem. Biophys. Res. Commun. 320 (2004) 100–107.

[10] T. Akimoto, T. Ushida, S. Miyaki, H. Akaogi, K. Tsuchiya, Z. Yan, R.S. Williams, T. Tateishi, Mechanical stretch inhibits myoblast-to-adipocyte differentiation through Wnt signaling, Biochem. Biophys. Res. Commun. 329 (2005) 381–385.

[11] A. Takahashi, Y. Kureishi, J. Yang, Z. Luo, K. Guo, D. Mukhopadhyay, Y. Ivashchenko, D. Branellec, K. Walsh, Myogenic Akt signaling regulates blood vessel recruitment during myofiber growth, Mol. Cell. Biol. 22 (2002) 4803–4814.

[12] J.B. Hansen, R.K. Petersen, B.M. Larsen, J. Bartkova, J. Alsner, K. Kristiansen, Activation of peroxisome proliferator-activated receptor γ bypasses the function of the retinoblastoma protein in adipocyte differentiation, J. Biol. Chem. 274 (1999) 2386–2393.

[13] Y. Lee, C. Ahn, J. Han, H. Choi, J. Kim, J. Yim, J. Lee, P. Provost, O. Radmark, S. Kim, V.N. Kim, The nuclear RNase III Drosha initiates microRNA processing, Nature 425 (2003) 415–419.

[14] T. Takahashi, B. Lord, P.C. Schulze, R.M. Fryer, S.S. Sarang, S.R. Gullans, R.T. Lee, Ascorbic acid enhances differentiation of embryonic stem cells into cardiac myocytes, Circulation 107 (2003) 1912–1916.

[15] M. Buckingham, L. Bajard, T. Chang, P. Daubas, J. Hadchouel, S. Meilhac, D. Montarras, D. Rocancourt, F. Relaix, The formation of skeletal muscle: from somite to limb, J. Anat. 202 (2003) 59–68.

[16] M. Crescenzi, D.H. Crouch, F. Tato, Transformation by myc prevents fusion but not biochemical differentiation of C2C12 myoblasts: mechanisms of phenotypic correction in mixed culture with normal cells, J. Cell Biol. 125 (1994) 1137–1145.

[17] S. Russo, D. Tomatis, G. Collo, G. Tarone, F. Tato, Myogenic conversion of NIH3T3 cells by exogenous MyoD family members: dissociation of terminal differentiation from myotube formation, J. Cell Sci. 111 (1998) 691–700.

[18] I.H. Park, J. Chen, Mammalian target of rapamycin (mTOR) signaling is required for a late-stage fusion process during skeletal myotube maturation, J. Biol. Chem. 280 (2005) 32009–32017.

[19] A. Pisconti, S. Brunelli, M. Di Padova, C. De Palma, D. Deponti, S. Baesso, V. Sartorelli, G. Cossu, E. Clementi, Follistatin induction by nitric oxide through cyclic GMP: a tightly regulated signaling pathway that controls myoblast fusion, J. Cell Biol. 172 (2006) 233–244.

[20] V. Jacquemin, D. Furling, A. Bigot, G.S. Butler-Browne, V. Mouly, IGF-1 induces human myotube hypertrophy by increasing cell recruitment, Exp. Cell Res. 299 (2004) 148–158.

[21] P.K. Rao, R.M. Kumar, M. Farkhondeh, S. Baskerville, H.F. Lodish, Myogenic factors that regulate expression of muscle-specific microRNAs, Proc. Natl. Acad. Sci. USA 103 (2006) 8721–8726.

[22] A. Nakashima, T. Katagiri, M. Tamura, Cross-talk between Wnt and bone morphogenetic protein 2 (BMP-2) signaling in differentiation pathway of C2C12 myoblasts, J. Biol. Chem. 280 (2005) 37660–37668.

[23] Y.J. Kim, M.H. Lee, J.M. Wozney, J.Y. Cho, H.M. Ryoo, Bone morphogenetic protein-2-induced alkaline phosphatase expression is stimulated by Dlx5 and repressed by Msx2, J. Biol. Chem. 279 (2004) 50773–50780.

[24] A. Krek, D. Grun, M.N. Poy, R. Wolf, L. Rosenberg, E.J. Epstein, P. MacMenamin, I. da Piedade, K.C. Gunsalus, M. Stoffel, N. Rajewsky, Combinatorial microRNA target predictions, Nat. Genet. 37 (2005) 495–500.

Glia Maturation Factor-γ Is Preferentially Expressed in Microvascular Endothelial and Inflammatory Cells and Modulates Actin Cytoskeleton Reorganization

Koji Ikeda, Ramendra K. Kundu, Shoko Ikeda, Miyuki Kobara, Hiroaki Matsubara, Thomas Quertermous

Abstract—Actin cytoskeleton reorganization is a fundamental process for actin-based cellular functions such as cytokinesis, phagocytosis, and chemotaxis. Regulating actin cytoskeleton reorganization is therefore an attractive approach to control endothelial and inflammatory cells function and to treat cardiovascular diseases. Here, we identified glia maturation factor-γ (GMFG) as a novel factor in actin cytoskeleton reorganization and is expressed preferentially in microvascular endothelial and inflammatory cells. During mouse embryogenesis, GMFG was expressed predominantly in blood islands of the yolk sac, where endothelial and hematopoietic cells develop simultaneously. In endothelial cells, GMFG was colocalized with F-actin in membrane ruffles and was associated with F-actin assessed by actin co-sedimentation assay. Interestingly, GMFG was phosphorylated at N-terminal serine, and its phosphorylation was enhanced by coexpression of dominant active Rac1 and Cdc42. Furthermore, a pseudophosphorylated form of GMFG (GMFG-S2E) demonstrated higher association with F-actin. Stable expression of GMFG-S2E remarkably enhanced stimulus-responsive lamellipodia and subsequent membrane ruffle formation in HeLa cells presumably through its interaction with Arp2/3 complex. Expression of GMFG enhanced actin-based cellular functions such as migration and tube-formation in endothelial cells. Moreover, we found that GMFG expression was significantly increased in a cardiac ischemia/reperfusion model where inflammation and angiogenesis take place actively. Taken together, our findings define a novel pathway in the regulation of actin-based cellular functions. Regulating GMFG function may provide a novel approach to modulate the pathophysiology of cardiovascular diseases. (***Circ Res.* 2006;99:424-433.**)

Key Words: actin cytoskeleton reorganization ■ actin-based cellular function ■ microvascular endothelial cells ■ inflammatory cells

Endothelial cells, composing a single layer inside the blood vessels, play critical roles in a variety of physiological and pathological phenomena such as angiogenesis and atherosclerosis. Because genes specifically or preferentially expressed in endothelial cells are likely to play a crucial role for their unique physiology, we performed a series of microarray studies aimed at isolating unique endothelial cell genes. We successfully identified several genes specifically or preferentially expressed in endothelial cells.[1] Among these genes, glia maturation factor-γ (GMFG) demonstrated a very unique expression pattern: expressed only in microvascular endothelial cells but not by endothelial cells from other vascular beds or nonendothelial cells. These results urged us to further analyze GMFG function in endothelial cells.

GMFG was initially identified as a molecule that was highly similar to glia maturation factor-β.[2] However, GMFG is expressed neither in brain, neuronal cells, nor glia cells, and its function is entirely unknown. We found the amino acid sequence of GMFG is similar to cofilin, a key regulator of actin cytoskeleton reorganization and thus analyzed GMFG function in actin cytoskeleton reorganization. Actin cytoskeleton reorganization is clearly an essential factor for a large number of cellular processes such as cytokinesis, endocytosis, and chemotaxis.[3,4] In response to extracellular stimuli, motile protrusions of plasma membrane, called lamellipodia or filopodia are created by the continuous polarized growth and turnover of actin filaments, leading to actin-based cellular functions.[3,4] Deficient actin cytoskeleton reorganization causes impaired endothelial cell migration, reduces macrophage phagocytosis, and results in defective lymphocyte development and activation.[5–7] Actin cytoskeleton reorganization is thus pivotal for angiogenesis and immune system function.

Actin dynamics is regulated by an elaborate mechanism that involves many actin-associated molecules. In resting

Original received March 26, 2006; revision received July 12, 2006; accepted July 13, 2006.

From the Donald W. Reynolds Cardiovascular Clinical Research Center (K.I., R.K.K., T.Q.), Division of Cardiovascular Medicine, Stanford University School of Medicine, Calif; Department of Clinical Pharmacology (M.K.), Kyoto Pharmaceutical University, Japan; and Department of Cardiology and Vascular Regenerative Medicine (K.I., S.I., H.M.), Kyoto Prefectural University of Medicine, Japan.

Correspondence to Koji Ikeda, Department of Cardiology and Vascular Regenerative Medicine, Kyoto Prefectural University of Medicine, Kyoto, Kawaramachi-Hirokoji, Kamigyo-ku, Kyoto 602-8566, Japan. E-mail ikedak@koto.kpu-m.ac.jp

Circulation Research is available at http://circres.ahajournals.org DOI: 10.1161/01.RES.0000237662.23539.0b

cells, actin monomers are kept from polymerizing by monomer-binding protein such as thymosin-β4, twinfilin, and profilin.[3,8] Capping proteins such as CapZ and gelsolin are also required to maintain a pool of actin monomers by capping free barbed ends of actin filaments, resulting in blocking the addition of actin monomers to the barbed ends. Extracellular stimuli activate Wiscott–Aldrich syndrome protein (WASP) and WASP family verprolin homologous (WAVE) largely through small GTPases, Rac, and Cdc42. Activated WASP/WAVE further activates the actin-related protein 2/3 (Arp2/3) complex to nucleate actin polymerization by serving as a template for the formation of new actin filaments.[3] During the active actin polymerization at the barbed ends, actin-depolymerization takes place as a result of the function of cofilin at the pointed ends, which replenishes the actin monomer pool.[4,9,10]

Recently, it has been reported that WAVE2 is expressed predominantly in endothelial cells during embryogenesis and that its deficiency causes embryonic lethality because of hemorrhage.[5] WAVE2$^{-/-}$ mice demonstrated decreased sprouting and branching of endothelial cells from existing vessels during angiogenesis. Furthermore, the formation of lamellipodia and capillaries was severely impaired in WAVE2$^{-/-}$ endothelial cells. These results indicate that proper regulation of actin cytoskeleton reorganization is critical for endothelial cell migration and angiogenesis.

Here, we report the characterization of GMFG, a novel factor in actin cytoskeleton reorganization, preferentially expressed in microvascular endothelial cells and inflammatory cells. GMFG remarkably enhanced stimulus-responsive lamellipodia formation, and its function was likely regulated via phosphorylation of N-terminal serine under the control of small GTPases. Overexpression of GMFG enhanced actin-based cellular functions such as cell motility and tube-formation in endothelial cells. Regulating GMFG function may provide a unique opportunity to control actin cytoskeleton reorganization in microvascular endothelial and inflammatory cells and, therefore, to modulate the pathophysiology of ischemic and inflammatory diseases.

Materials and Methods

DNA Constructs

Full-length human GMFG and cofilin were obtained by RT-PCR using cDNA prepared from human microvascular endothelial cells. A *Bam*HI site was created before the stop codon by adding 5′-GGATCC-3′ at the beginning of reverse primer. Mutagenesis was performed by creating point mutations in the forward primers that cause a missense mutation of serine into alanine or glutamic acid. These cDNAs were subcloned into pCR-blunt II-TOPO vector (Invitrogen) and the nucleotide sequence was validated. Fragments cut out with *Eco*RI and *Bam*HI were subcloned into p3XFLAG-CMV-14 expression vector (Sigma) to obtain the expression constructs.

Reverse-Transcription PCR

Total RNA was isolated from cells cultured in growth media, followed by cDNA synthesis. Primers used for GMFG amplification were of 100% match for both human and bovine GMFG, 5′-GACTCCCTGGTGGTGTG -3′ and 5′-TACAACGAAAGAAAGACAACTT-3′. Twenty-eight PCR cycles with annealing temperature at 57°C were performed for amplification of both GMFG and GAPDH.

In Situ Hybridization

Whole-mount in situ hybridization was performed using digoxigenin-labeled cRNA as previously described.[11] After all procedures, embryos were embedded in OCT and snap-frozen by immersion in ethanol cooled on dry ice. Sections were counterstained with eosin.

Transfection and Immunofluorescence Study

Expression constructs were transfected into bovine aortic endothelial cells (BAECs) or HeLa cells using Lipofectamine 2000 (Invitrogen) according to the recommendations of the manufacturer. Cells were plated into chamber slides 24 hours after transfection and further incubated for 24 hours followed by staining with Alexa Fluor3–phalloidin (Molecular Probes) and FITC-anti–FLAG M2 antibody (Sigma). After mounting, cells were observed under a fluorescent microscope (Axioplan 2; Zeiss).

Cell Culture

BAECs in passage 4 to 7 were used for all experiments. Human microvascular endothelial cells were obtained from Clonetics and cultured in EGM-2MV media. To generate stable transfectants, HeLa cells underwent the selection in the growth media containing 300 μg/mL G418, and pooled clones were used for experiments. Expression of transgenes was confirmed by RT-PCR using vector-specific primers, 5′-AAGCTTGCGGCCGCGAATTC-3′ and 5′-TTTGTAGTCAGCCCGGGATCC. The nucleotide sequence of the PCR product was validated by direct sequencing. Recombinant protein expression was confirmed by immunoblotting using anti–FLAG M2 antibody (Stratagene). For epidermal growth factor (EGF) stimulation experiment, HeLa cells were cultured in serum-free media for 24 hours, followed by stimulation with 100 ng/mL or 1000 ng/mL EGF (Sigma) for 5 minutes. Cells were fixed with 4% paraformaldehyde and observed under a phase-contrast microscope (TE 2000 U; Nikon).

Metabolic Labeling

Cells were labeled by incubating with 1 mCi/mL of P^{32}-phosphate (Perkin Elmer) in phosphate-free DMEM containing 10% dialyzed FBS (Invitrogen) for 4 hours. Immunoprecipitated recombinant proteins were run on SDS-PAGE and then transferred onto polyvinylidene difluoride (PVDF) membrane. Phosphorylated proteins were visualized by autoradiography.

Actin Co-Sedimentation Assay

BAECs transiently transfected with cofilin or GMFG were collected in ice-cold PBS and resuspended in binding buffer (10 mmol/L imidazole, ph 7.2, 75 mmol/L KCl, 5 mmol/L $MgCl_2$, 1 mmol/L EGTA, 0.5 mmol/L dithiothreitol [DTT], 0.2 mmol/L ATP, 1 mmol/L NaF, 0.5 mmol/L Na_3VO_4, and protease inhibitor cocktail). Nonmuscle actin was obtained from Cytoskeleton Inc and polymerized according to the instructions of the manufacturer. Cell lysates were prepared with three bursts of sonication followed by ultracentrifugation at 150 000g, and then the supernatants were incubated in the presence or absence of 5.5 μmol/L F-actin at room temperature for 30 minutes. The reaction mixtures underwent ultracentrifuge at 150 000g for 30 minutes to precipitate F-actin. Supernatants were carefully collected and pellets were resuspended in exactly the same volume of binding buffer as the supernatants. Proteins of interest were detected by immunoblotting, and the amount of sedimentation was assessed by densitometry analysis.

Modified Boyden Chamber Assay and Two-Dimensional Tube-Formation Assay

Modified Boyden chamber assay and tube-formation assay were performed as previously described.[12]

Arp2/3 Complex–Binding Assay

Arp 2/3 complex in cell lysates was immunoprecipitated with anti-ARPC2 antibody (Upstate). Coprecipitation of GMFG was detected by immunoblotting using anti–FLAG M2 antibody.

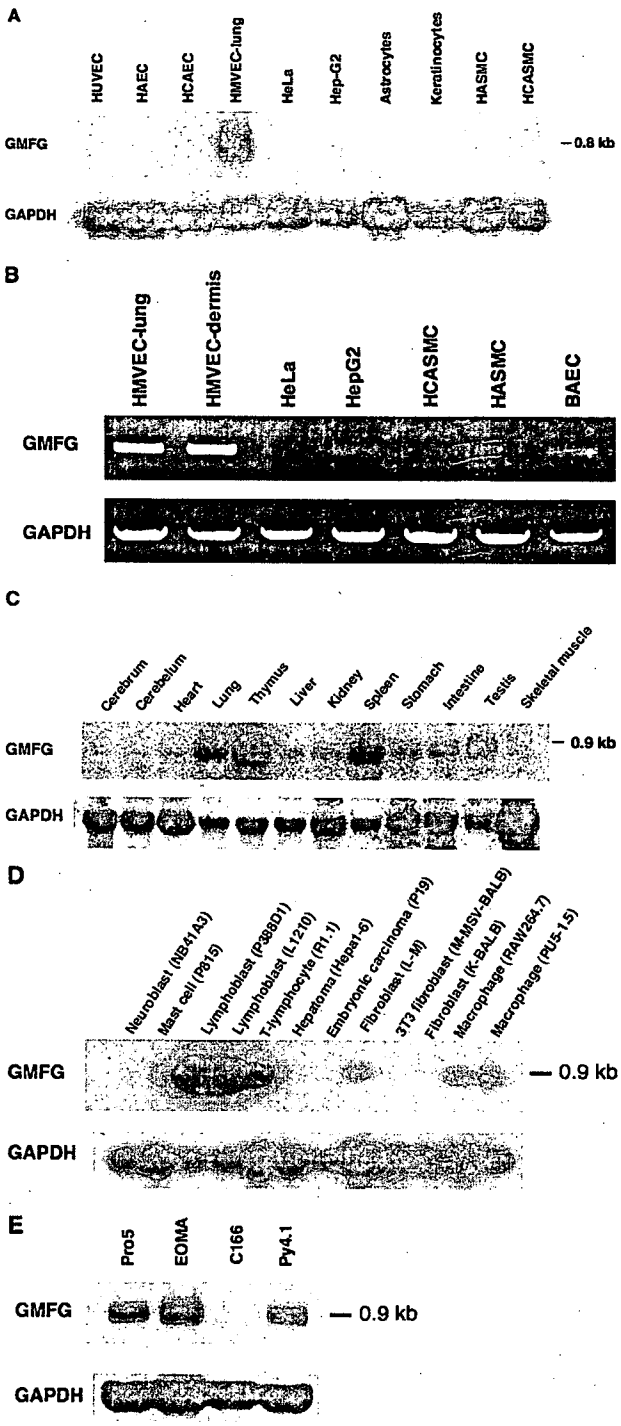

Figure 1. GMFG is expressed in specific types of cells. A, Northern blot analysis of GMFG in primary cultured human endothelial cells and other cultured human cells. Cells examined were human umbilical vein endothelial cells (HUVECs), human aortic endothelial cells (HAECs), human coronary artery endothelial cells (HCAECs), human lung microvascular endothelial cells (HMVEC-lung), human epithelial tumor cells (HeLa), human hepatoma cells (Hep-G2), human astrocytes, human keratinocytes, human aortic smooth muscle cells (HASMCs), and human coronary artery smooth muscle cells (HCASMCs). B, RT-PCR analysis of GMFG. HMVEC from dermis expressed GMFG as much as HMVEC-lung, whereas bovine aortic endothelial cells (BAECs) expressed minimal amount of GMFG. C, Northern blot analysis of GMFG in mouse tissues. D, Northern blot analysis of GMFG in mouse cell line MTN blot (BD Clontech). E, Northern blot analysis of GMFG in mouse endothelial cell lines. Cells examined were Pro5 (endothelial-like cells isolated from embryonic yolk sac of a normal mouse), EOMA (mouse endothelioma cell line), py4.1 (derived from microvessels of an SV40T transgenic mouse), and C166 (isolated from embryonic yolk sac of a protooncogene transgenic mouse).

Mouse Ischemia/Reperfusion Model

The mice underwent pre-anesthesia with a single intraperitoneal injection of sodium pentobarbital (25 mg/kg). Following endotracheal intubation, a thoracotomy incision through the fourth intercostal space was made. The left anterior descending (LAD) coronary artery was occluded for 30 minutes then reperfused for 24 hours. At the end of the experiments, the chest was opened and the left ventricles were immediately excised followed by snap freezing for RNA extraction.

Statistics

Differences between groups were analyzed using student's t test; $P<0.05$ was considered significant. Data are presented as mean±SE as indicated.

Results

Glia Maturation Factor-γ Is Preferentially Expressed in Microvascular Endothelial and Inflammatory Cells

During a series of microarray studies aimed at isolating unique endothelial cell genes, we identified previously uncharacterized GMFG as being expressed only in microvascular endothelial cells derived from human lung but not by endothelial cells from other vascular beds or nonendothelial cells (Figure 1A). Amino acid sequence of GMFG is highly conserved among species, eg, 95% homology between human and mouse and 98% homology between human and bovine. GMFG was also expressed in dermal microvascular cells as much as in lung microvascular endothelial cells, and minimal expression was observed in hepatoma cells, vascular smooth muscle cells, and endothelial cells from bovine aorta, assessed by RT-PCR (Figure 1B). The primers used were of 100% match for both human and bovine GMFG. In adult mouse tissues, GMFG was expressed abundantly in thymus and spleen as well as in lung (Figure 1C). We found that GMFG was expressed in inflammatory cells such as lymphoblasts, T lymphocytes, and macrophages, a finding that is consistent with its high expression in thymus and spleen (Figure 1D). Mouse endothelial cell lines derived from normal yolk sac (Pro5), endothelioma (EOMA), and microvessels of an SV40T transgenic mouse (py4.1) also expressed GMFG (Figure 1E).

During mouse embryogenesis, GMFG was expressed as early as embryonic day 9.5 (e9.5) (Figure 2A), predominantly in blood islands of the yolk sac, in endothelial and hematopoietic cells, and possibly in the angioblast precursors to these lineages (Figure 2B through 2G). Negative control study using sense RNA probe did not show such a significant hybridization signals (Figure I in the online data supplement, available at http://circres.ahajournals.org). These results suggest that GMFG has a function in embryonic vasculogenesis as well as in hematopoiesis and that its expression might be well preserved during differentiation, which could account

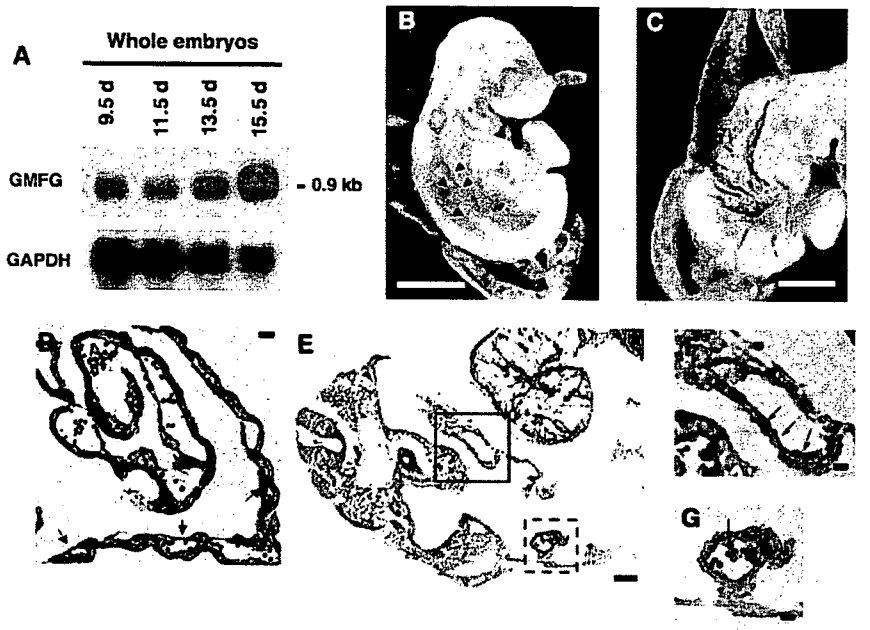

Figure 2. GMFG expression during mouse embryogenesis. A, Northern blot analysis of GMFG in whole embryos of e9.5, e11.5, e13.5, and e15.5. B, Whole-mount in situ hybridization of GMFG in e9.5d embryo. GMFG was expressed in dorsal aorta and intersomitic artery as indicated by arrowheads. C, GMFG was expressed predominantly in the yolk sac and demonstrated a spotty staining pattern. D, E, F, and G, Sections of embryo from the whole-mount in situ hybridization. GMFG expression was observed in blood islands of the yolk sac as indicated by arrows (D). GMFG was also expressed in endothelial cells and hematopoietic cells in the body (E through G). High-power views of the boxed area in E, with the solid line (F) and the broken line (G), are shown. Arrows indicate endothelial cells in F and hematopoietic cells in G. Bars are 500 μm (B and C), 100 μm (D and E), and 20 μm (F and G).

for the unique GMFG expression in microvascular endothelial cells and hematopoietic lineage-derived cells in adults.

GMFG Has a Similar Structure to Cofilin and Is Associated With F-Actin

The amino acid sequence of GMFG demonstrated significant similarity to cofilin, a key regulator of actin cytoskeleton reorganization (Figure 3A). Cofilin plays critical roles in actin dynamics through its actin-severing and actin-depolymerizing activities. Therefore, we determined to analyze GMFG function in actin cytoskeleton reorganization. We first examined the subcellular localization of GMFG and cofilin in bovine aortic endothelial cells (BAECs). Recombinant cofilin and GMFG localized preferentially in the F-actin–rich structures in membrane ruffles as well as in nucleus (Figure 3B). Furthermore, native GMFG in human microvascular endothelial cells also demonstrated colocalization with F-actin in membrane ruffles (Figure 3C). These results suggest that GMFG may play a role in actin dynamics at the leading edge of cells. We then examined if GMFG is associated with F-actin using actin co-sedimentation assay. Cell lysates from GMFG or cofilin-expressing BAECs were incubated with F-actin followed by ultracentrifugation to precipitate F-actin. Significant co-sedimentation of GMFG in the pellet was detected by immunoblotting as well as of cofilin, indicating that GMFG is associated with F-actin (Figure 3D).

GMFG Is a Phosphoprotein, and Its Phosphorylation Is Enhanced by Coexpression of Dominant Active Rac and Cdc42

Because cofilin function is tightly regulated by phosphorylation of a single N-terminal serine residue, and GMFG also has N-terminal serines at the second (Ser2) and fourth (Ser4) position (Figure 3A), we explored their possible phosphorylation in GMFG. Expression constructs of wild-type GMFG (GMFG-WT) and GMFG mutants, in which Ser2 and/or Ser4 were replaced with alanine, were transfected into BAECs. Metabolic labeling of BAECs with P^{32}-phosphate revealed that GMFG was phosphorylated in cells, and replacing Ser2 and/or Ser4 with alanine completely abolished phosphorylation (Figure 4A). These results indicate that Ser2 and/or Ser4 are the phosphorylation sites and that both Ser2 and Ser4 are essential for GMFG phosphorylation. Of note, when incubated in serum-free media, phosphorylation of GMFG significantly diminished, suggesting that phosphorylation might be enhanced by soluble factors such as growth factors (Figure 4B).

Because small GTPases play central roles in actin cytoskeleton reorganization, we investigated the effect of small GTPases on GMFG phosphorylation. Coexpression of dominant active Rac1 and Cdc42 significantly enhanced GMFG phosphorylation, whereas dominant active RhoA did not (Figure 4C). These results suggest that GMFG function might be modified by Rac and Cdc42.

GMFG Association With F-Actin Is Regulated by Phosphorylation of N-Terminal Serine

To explore the effect of phosphorylation on GMFG function, we prepared a series of GMFG mutant expression constructs in which Ser2 and/or Ser4 were replaced with alanine (SA) (nonphosphorylated mutant) or glutamic acid (SE) (pseudophosphorylated mutant). Cell lysates of BAECs expressing GMFG-WT or GMFG mutants were incubated with F-actin, and their co-sedimentation with F-actin was detected by immunoblotting. When incubated in the absence of F-actin, only minimal sedimentation was observed except in the cases of GMFG-S2/4A and GMFG-S2A where sedimentation of some insoluble fractions in the absence of F-actin were consistently observed in 3 independent experiments (Figure 4). We subtracted the background sedimentation (in the absence of F-actin) from the co-sedimentation with F-actin and regarded it as the sedimentation associated with F-actin. Interestingly, GMFG-S2/4E and especially GMFG-S2E dem-

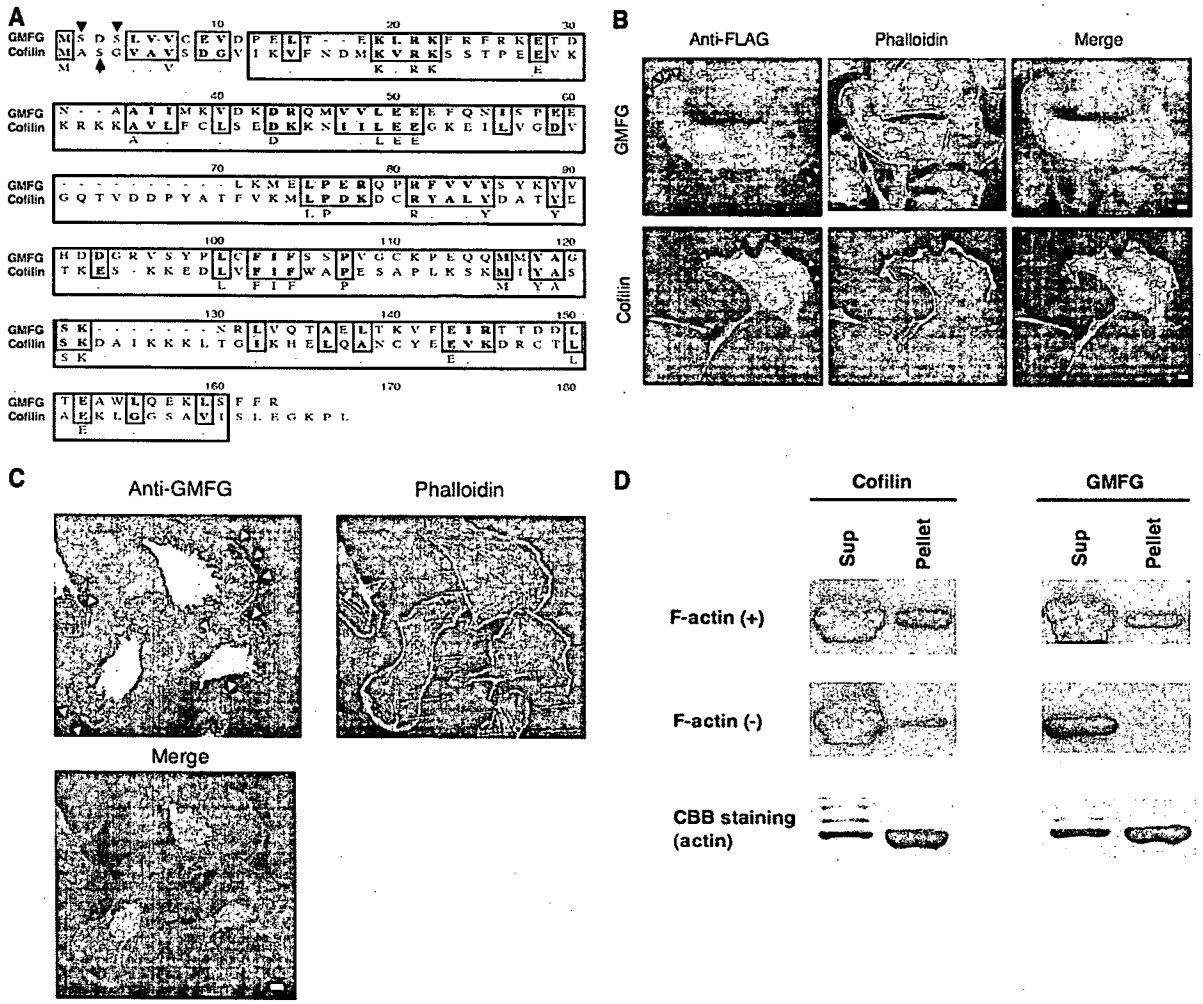

Figure 3. GMFG has a similar structure to colilin and is associated with F-actin. A, GMFG demonstrates 39% similarity to cofilin and has a similar actin-depolymerizing factor homology domain to cofilin as surrounded by a solid line. Similar amino acids between GMFG and cofilin are highlighted. Cofilin function is tightly regulated by phosphorylation of the N-terminal serine indicated by the arrow. GMFG has serines at second and fourth position as indicated by arrowheads. B, Immunostaining of F-actin and FLAG-tagged recombinant GMFG or cofilin in bovine aortic endothelial cells (BAECs). Significant localization in the forward periphery F-actin–rich structures was observed in both GMFG and cofilin as indicated by arrowheads. C, Immunostaining of F-actin and native GMFG in HMVEC. Significant localization of GMFG in the forward periphery F-actin–rich structures was observed as indicated by arrowheads. Bars=10 μm. D, Cell lysate from BAECs expressing cofilin or GMFG was incubated with F-actin followed by ultracentrifugation. Supernatants (S) and resuspended pellets (P) were run on SDS-PAGE, and the proteins of interest were detected by immunoblotting. F-actin was successfully precipitated in pellets visualized by Coomassie brilliant blue (CBB) staining. Similar results were obtained by 2 independent experiments.

onstrated significantly higher association with F-actin than other GMFG mutants or GMFG-WT, suggesting that phosphorylation of Ser2 but not Ser4 enhances GMFG association with F-actin. To exclude the possibility that replacement of N-terminal serine with alanine caused inappropriate protein folding or localization, we examined the subcellular localization of recombinant GMFG-S2/4A, GMFG-S2A, and GMFG-S4A. They demonstrated similar subcellular localization to GMFG-WT, suggesting that replacement of N-terminal serine with alanine did not cause inappropriate protein folding or localization (Figure 5B).We also confirmed that recombinant GMFG mutant of which serine(s) was replaced with glutamic acid(s) demonstrated proper subcellular localization (data not shown). It is intriguing that although the affinity of GMFG and cofilin for F-actin is regulated by phosphorylation of the N-terminal serine, phosphorylation enhances GMFG binding, whereas it reduces cofilin binding to F-actin.

GMFG Is a Novel Factor in Actin Cytoskeleton Reorganization

Because cofilin directly affects actin filament turnover, we investigated the effects of GMFG on actin cytoskeleton reorganization. Somewhat surprisingly, HeLa cells transiently transfected with GMFG-WT or the pseudophosphorylated form of GMFG (GMFG-S2E) demonstrated no significant change in F-actin structure, whereas expression of wild-type cofilin (cofilin-WT) or the active form of cofilin (cofilin-S3A) significantly reduced F-actin structure (Figure 6A). These results suggest that GMFG does not have a significant actin-depolymerizing activity and may have a different function in actin dynamics from cofilin.

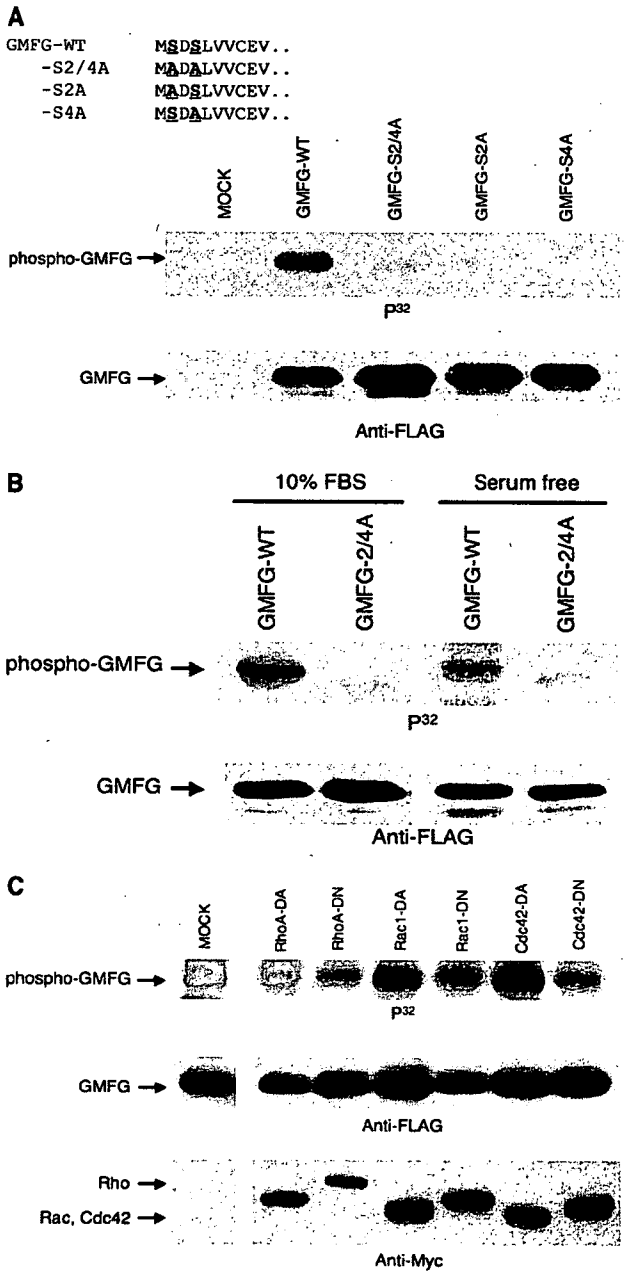

Figure 4. GMFG is a phosphoprotein. A, BAECs expressing the wild-type GMFG (GMFG-WT), GMFG mutants, or empty vector (MOCK) were labeled with P^{32}-phosphate. Immunoprecipitated GMFG was run on SDS-PAGE and the phosphorylated GMFG was visualized by autoradiography. Whole GMFG expression was detected by immunoblotting using anti-FLAG M2 antibody. Results were confirmed by 3 independent experiments. B, BAECs expressing GMFG were incubated either in growth media or serum-free media for overnight followed by labeling with P^{32}-phosphate. C, GMFG was coexpressed with either dominant active (DA) or dominant negative (DN) form of Rho, Rac, and Cdc42 or empty vector (MOCK). Cells were labeled with P^{32}-phosphate, and GMFG phosphorylation was visualized by autoradiography. GMFG and small GTPase expressions were detected by immunoblotting using anti-FLAG M2 and anti-myc 9E10 antibody, respectively. Similar results were obtained by 3 independent experiments.

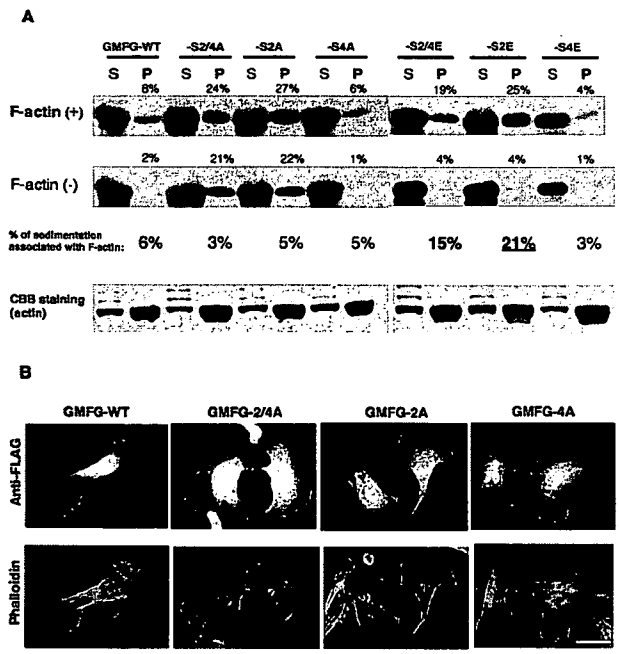

Figure 5. GMFG is associated with F-actin. A, Actin co-sedimentation assay was performed as described in Figure 2D. Pseudophosphorylation of Ser2 significantly enhanced GMFG association with F-actin. Similar results were obtained by 3 independent experiments. B, Immunostaining of recombinant GMFG-WT or GMFG mutants and F-actin in BAECs. Bar=50 μm.

We then generated HeLa cells stably expressing cofilin-WT, cofilin-S3A, GMFG-WT, GMFG-S2E, and GMFG-S4E. Because HeLa cells are the most widely used and the most-characterized cells for the research of actin cytoskeleton reorganization, we chose HeLa cells to analyze GMFG function in actin cytoskeleton reorganization. Stable expression of transgenes and recombinant proteins were confirmed by RT-PCR and immunoblotting respectively (data not shown). Large populations (≈30%) of cells stably expressing cofilin-S3A (HeLa/cofilin-S3A) demonstrated enhanced membrane ruffles formation under the basal culture condition, whereas none of the other stable transfectants demonstrated such a phenotype (Figure 6B and 6C).

On the other hand, when cells were stimulated with a low concentration (100 ng/mL) of EGF following the incubation in serum-free media for 24 hours, HeLa/GMFG-S2E demonstrated significant stimulus-responsive lamellipodia and subsequent ruffles formation (Figure 6D and 6E). HeLa/GMFG-WT also demonstrated less but significant stimulus-responsive lamellipodia formation with 100 ng/mL EGF treatment (Figure 6D and 6E). None of the other transfectants, including HeLa/MOCK, demonstrated such an effect. Stimulation with 1000 ng/mL EGF induced stimulus-responsive lamellipodia and subsequent ruffle formation in all stable transfectants (data not shown). These results suggest a significant role of GMFG in stimulus-responsive actin polymerization. Despite its structural similarity, GMFG appears to play a different role from cofilin in actin cytoskeleton reorganization. It has been reported that twinfilin, another actin-depolymerizing factor domain family protein, does not have actin-depolymerizing activity and functions in actin dynamics in clearly distinct manner from cofilin.[8] Moreover,

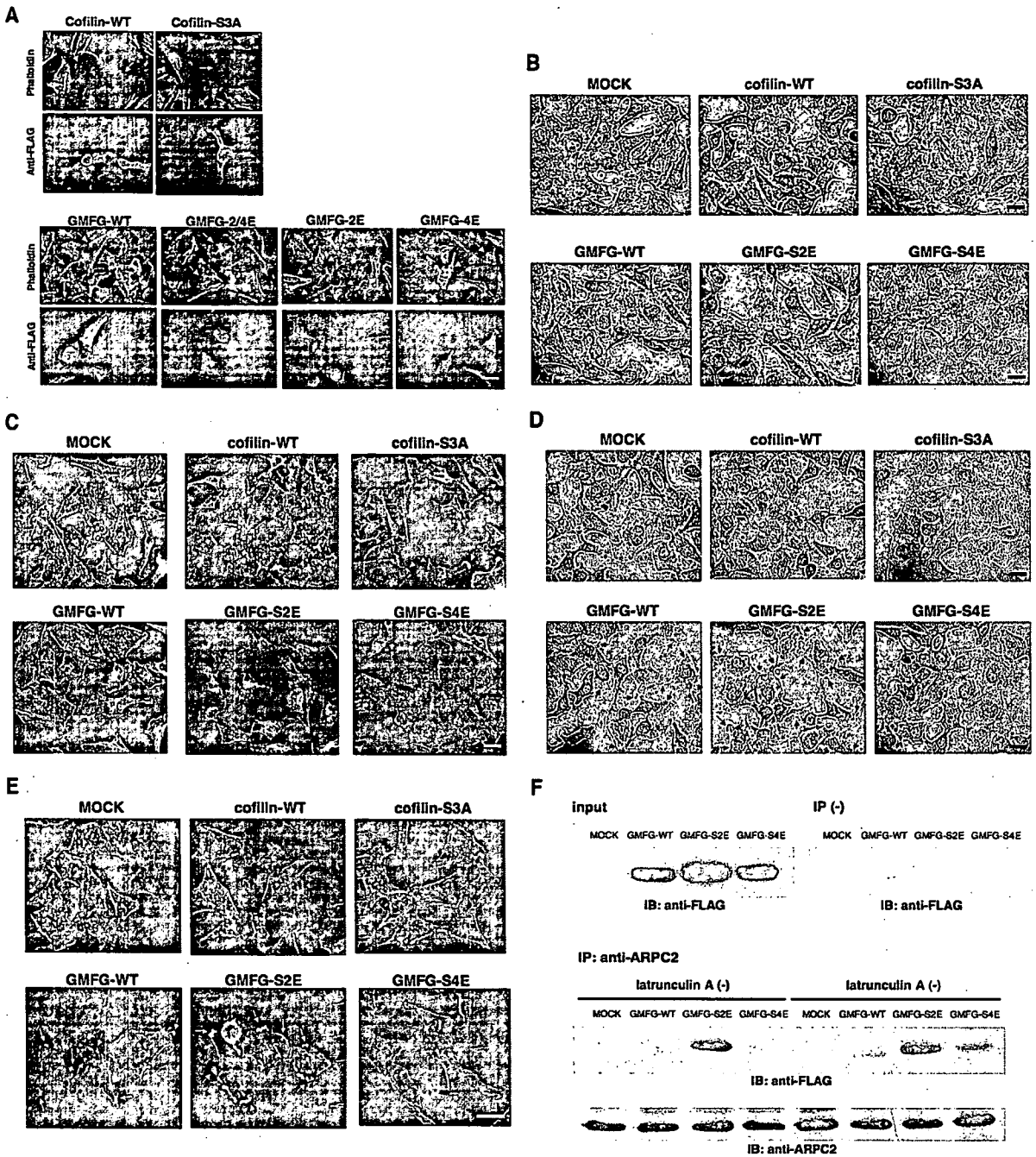

Figure 6. GMFG enhances stimulus-responsive lamellipodia formation, presumably through its interaction with Arp2/3 complex. A, F-actin and recombinant protein were visualized in HeLa cells expressing the protein of interest. Arrows indicate cells expressing the designated protein. B, Images of HeLa cells stably expressing the protein of interest under the basal culture condition by the phase-contrast microscopy. C, F-actin were visualized in HeLa cells under the same condition as in B. Arrows indicate the enhanced membrane ruffles formation. D, HeLa cells stably expressing the protein of interest were incubated in serum-free media for 24 hours, followed by stimulation with 100 ng/mL EGF. Stimulus-responsive lamellipodia and subsequent membrane ruffles formation are indicated by arrows. E, F-actin were visualized in HeLa cells under the same condition as in D. Arrows indicate the stimulus-responsive lamellipodia and subsequent membrane ruffles formation. Bars=40 μm. Similar results were obtained by 2 independent experiments. F, Arp2/3 complex in the cell lysate was immunoprecipitated with anti-ARPC2 antibody. Coprecipitation of GMFG with Arp2/3 complex was detected by immunoblotting. To exclude the potential nonspecific interactions from coprecipitation of actin filaments, 40 μmol/L latrunculin A was included in the immunoprecipitation reactions. Results were confirmed by 2 independent experiments.

Abp1p, an actin binding protein originally isolated from yeast, also has an actin-depolymerizing factor homology domain, but it binds to Arp2/3 complex and activates the actin nucleation, not actin depolymerization.[13]

To better understand the cellular mechanisms by which GMFG enhances stimulus-responsive lamellipodia formation, we investigated the possible interaction of GMFG with the Arp2/3 complex, a key regulator of stimulus-responsive actin

polymerization. Cell lysates expressing GMFG were incubated with anti–Arp2/3 complex subunit 2 (ARPC2) antibody, and coprecipitation of GMFG with ARPC2 was detected by immunoblotting. To exclude the potential nonspecific interactions from coprecipitation of actin filaments, 40 μmol/L latrunculin A was included in the immunoprecipitation reactions. Immunoblotting confirmed no detectable actin in the pellets (data not shown). GMFG was coprecipitated with ARPC2, suggesting GMFG interaction with Arp2/3 complex (Figure 6F). Of note, more GMFG-S2E was pulled down than GMFG-WT or GMFG-S4E, indicating that phosphorylation of Ser2 enhances GMFG interaction with the Arp2/3 complex (Figure 6F). These results suggest that in response to extracellular stimuli, GMFG might be phosphorylated at Ser2 through Rac and Cdc42, promoting its interaction with Arp2/3 complex as well as with F-actin, which then accelerates stimulus-responsive actin polymerization at the leading edge of cells. However, further analysis is certainly required to conclude its functional relevance with Rac and Cdc42. Given that even pseudophosphorylated form of GMFG required exogenous stimulus to modulate actin cytoskeleton reorganization, GMFG binding to Arp2/3 complex is not sufficient to initiate new actin polymerization.

GMFG Positively Regulates Actin-Based Cellular Functions

We then investigated GMFG functions in actin-based cellular functions in endothelial cells. As shown in Figure 1B, BAECs express only a minimal amount of GMFG, much less than in microvascular endothelial cells. Therefore, we used BAECs to examine the effect of GMFG overexpression on actin-based cellular functions. The majority of cells expressed the transgene 24 hours after transfection, as assessed by GFP-construct transfection (supplemental Figure II). BAECs overexpressing GMFG demonstrated significantly higher motility than mock-transfected BAECs (Figure 7A). Moreover, BAECs overexpressing GMFG demonstrated significantly enhanced tube formation on Matrigel as compared with the mock-transfected cells (Figure 7B). These results suggest that GMFG positively regulates actin-based cellular functions in endothelial cells, presumably through accelerating stimulus-responsive actin polymerization.

Finally, we examined GMFG expression in a cardiac ischemia/reperfusion model because both angiogenesis and inflammation play important roles in the pathophysiology of ischemic cardiovascular diseases. GMFG expression was significantly increased in the ischemia/reperfusion tissues (Figure 7C and 7D). Although further analysis, such as immunohistochemistry to clarify the cells express GMFG, is certainly needed to address GMFG function in the ischemia/reperfusion heart, this result suggests possible GMFG involvement in the pathophysiology of cardiovascular diseases.

Our data define a novel pathway in the regulation of actin cytoskeleton reorganization and actin-based cellular functions (Figure 7E). Given that inflammatory cells and endothelial cells have a close relationship and interact with each other in ischemic cardiovascular diseases, GMFG may play a role in the pathophysiology of such diseases.[14,15]

Discussion

GMFG is preferentially expressed in human microvascular endothelial cells but not in endothelial cells from other vascular beds. Given that microvascular endothelial cells are the most important cellular players in angiogenesis in adults and expression of GMFG enhanced migration and tube formation in BAECs, GMFG may play a role in angiogenesis in adults. During embryogenesis, GMFG is predominantly expressed in blood islands of the yolk sac, in which hematopoietic and endothelial lineages develop simultaneously in close proximity, suggesting GMFG functions in embryonic vasculogenesis as well as hematopoiesis. This may also well correlate with the unique GMFG expression in microvascular endothelial cells and inflammatory cells seen in adults. In support of this contention, a search of the database of microarray analysis at the National Center for Biotechnology Information revealed that GMFG is expressed in a variety of hematopoietic cells such as T cell, B cell, NK cell, monocyte, and dendritic cell, as well as hematopoietic progenitor cells including $CD34^+$ and $CD105^+$ bone marrow cells, which may give rise to endothelial progenitor cells.[16,17]

Our findings demonstrated that GMFG plays a significant role in actin cytoskeleton reorganization distinct from cofilin, despite structural similarity. Stable expression of the pseudophosphorylated form of GMFG remarkably enhanced stimulus-responsive lamellipodia and subsequent membrane ruffles formation, presumably through interaction with Arp2/3 complex. In response to extracellular stimuli, active Rac and Cdc42 might activate GMFG via phosphorylation of Ser2 as well as WASP/WAVE. Binding of phosphorylated GMFG to the Arp2/3 complex might accelerate stimulus-responsive actin polymerization cooperating with active WASP/WAVE, resulting in enhanced actin-based cellular functions. However, further analysis is required to verify this hypothesis.

Of note, the pseudophosphorylated form of GMFG did not affect actin cytoskeleton reorganization in HeLa cells under basal culture conditions, although it remarkably enhanced stimulus-responsive lamellipodia formation. These results suggest that binding of GMFG to Arp2/3 complex is not sufficient to initiate new actin polymerization, but once Arp2/3 complex is activated by other activator such as WASP/WAVE, GMFG may enhance Arp2/3 complex-induced actin polymerization. Therefore, GMFG may enhance actin-based cellular functions only in the presence, and under the control, of endogenous stimulators such as growth factors and cytokines. In this regard, GMFG may be a good target for gene therapy because unexpected adverse effect caused by dysregulated transgene function is a considerable concern for the clinical application of gene therapy.

Our results indicate that GMFG is a novel factor in actin cytoskeleton reorganization and that it modulates actin-based cellular function in microvascular endothelial cells, inflammatory cells, and possibly hematopoietic progenitor cells. Because these cells are essential players in angiogenesis, vasculogenesis, and immune system function, and each of them plays specific roles in ischemic cardiovascular diseases, we believe that further analysis of GMFG will provide new insights into the molecular mechanisms of these diseases and

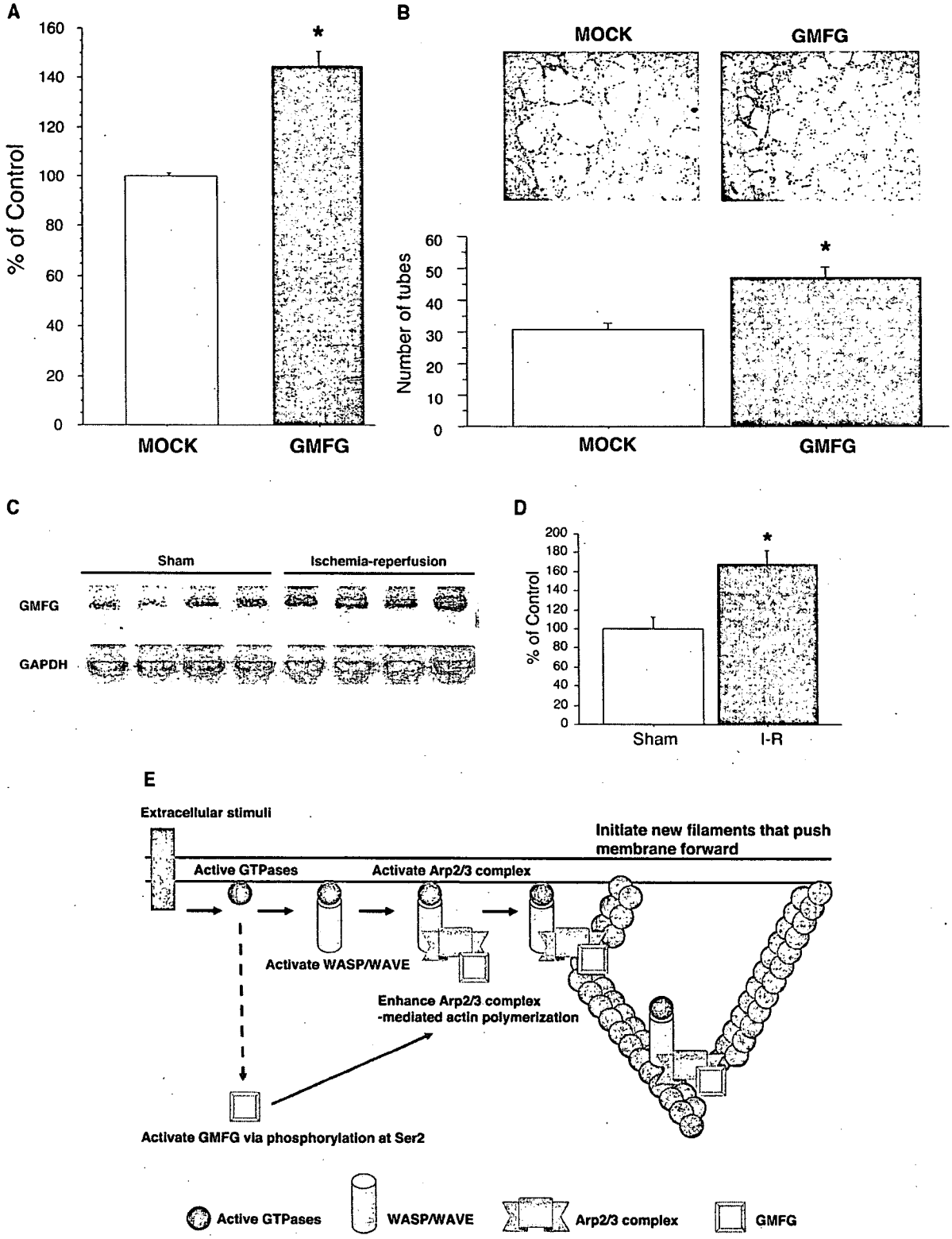

Figure 7. GMFG enhances actin-based cellular functions in endothelial cells. A, Cell motility of BAECs transiently transfected with GMFG or empty vector was examined by modified Boyden chamber assay (n=3). BAECs expressing GMFG demonstrated more motility than mock-transfected cells (*$P<0.0001$ vs MOCK). B, BAECs transfected with GMFG or empty vector were plated on Matrigel and incubated for 60 hours. Their tube-formation capacity was quantified by the number of tubes counted in 5 independent fields. BAECs expressing GMFG demonstrated significantly enhanced tube-formation capacity than mock-transfected cells (*$P<0.005$ vs MOCK) (n=2). C, Northern blot analysis of GMFG in the left ventricles from sham-operated (sham) or ischemia/reperfusion (I-R) model mice. D, Quantitative analysis of GMFG expression corrected by GAPDH. GMFG expression in ischemia/reperfusion left ventricles was significantly higher than in sham control (*$P<0.02$ vs sham control). E, Schematic diagram of GMFG pathway in actin dynamics.